https://doi.org/10.5194/wes-2024-144
Preprint. Discussion started: 21 November 2024

eawe european academy of wind energy
Open Access WIND ENERGY SCIENCE DISCUSSIONS

A multi-objective Economic Nonlinear Model Predictive Controller for Power and Platform Motion on Floating Offshore Wind Turbines

Luca Pustina[1], Francesco Biral[2], Enrico Bertolazzi[2], and Jacopo Serafini[3]

[1]Department of Mechanical and Aerospace Engineering, Sapienza University of Rome, Italy.
[2]Department of Industrial Engineering, University of Trento, Trento, Italy.
[3]Department of Civil, Computer Science, and Aeronautical Technologies Engineering, Roma Tre University, Rome, Italy.

Correspondence: Luca Pustina (luca.pustina@uniroma1.it), Francesco Biral (francesco.biral@unitn.it), Enrico Bertolazzi (enrico.bertolazzi@unitn.it), and Jacopo Serafini (serafini@uniroma3.it)

Abstract. A main target of the wind energy industry is the reduction of the Levelized Cost of Energy, especially for the emerging sector of floating turbines. An Economic Nonlinear Model Predictive Controller is developed to maximise power and reduce longitudinal motion, increasing revenues, and reducing capital and operating expenses. A novel comprehensive nonlinear Reduced Order Model of floating turbines is developed to predict platform motion, rotor thrust, aerodynamic power, and generator temperature. A grey-box approach and a black-box approach to platform modelling have been successfully validated and compared, identifying pros and cons. Then, the model is used in a constrained optimisation problem that computes the control action. The objectives are maximising aerodynamic power and reducing longitudinal nacelle velocity under realistic constraints (including bounds on rotor thrust, generator temperature, and platform velocities). The controller performance and robustness are assessed using a wide set of realistic wind and sea state load cases. Significant higher power production and a lower longitudinal platform motion concerning the standard NREL reference controller are achieved by adopting the multi-objective ENMPC. Finally, considering the difficulty in predicting the sea diffraction forces and the incoming wind, the performances are positively verified in the absence of that information.

1 Introduction

Reducing greenhouse gas emissions is the key to slowing and finally stopping climate change. The IPCC reports Masson-Delmotte et al. (2021a, b) show that a rapid and radical paradigm change is necessary to avoid the most catastrophic consequences. The shift to renewable energy from fossil fuels is considered to be the main driver of this change.

Concerning wind energy, the IRENA roadmap for 2050 VV.AA. (2019b) envisages a sixfold growth of the new annual installations compared to 2018 levels. This goal is only achievable by the strong growth of offshore wind. In fact, offshore wind is subject to minor restrictions with respect to its onshore counterpart, which is limited by public acceptance and logistical problems and the need for abundant wind and wide spaces. Instead, offshore farms take advantage of abundant and steady wind, fewer public acceptance issues, minor space value, and the possibility of installing larger turbines without particular transportation issues.

https://doi.org/10.5194/wes-2024-144
Preprint. Discussion started: 21 November 2024

eawe european academy of wind energy
Open Access WIND ENERGY SCIENCE DISCUSSIONS

Since the beginning of this century, offshore wind energy has experienced exponential growth. However, up to a year ago, the projects were limited to the North Sea, the Baltic Sea, and the Yellow Sea. In fact, since all farms were fixed foundation types, they required marine regions with a maximum depth of 60 m. To allow the exploitation of many sea zones with deeper water, in recent years, the possibility of realising floating offshore wind turbines (FOWTs) has been increasingly explored. This process quickly brought the FOWTs from the first small single demonstrator off the Apulia coast (Italy) in 2007, to progressively larger turbines, small farms of utility-scale wind turbines VV.AA. (2022), and finally to the request of authorisation of the first utility-scale farms Durakovic (2017). Although this process seems now unstoppable, many technical issues remain (see table 1 from James and Ros (2015) for a relatively old but still valid analysis of the main technical barriers), leaving much room for improvements in FOWT.

Technical challenge	Cost reduction potential	Urgency	IP sensitivity
Platform size & weight	2.7	2.4	2.8
Installation procedures	2.5	2.2	1.8
Port-side O&M (major repair procedures)	2.3	2.2	1.0
Floating substations/transformer modules	2.3	2.0	2.0
Advanced control systems for floating WTGs	2.2	2.2	2.6
Mooring design & installation	2.2	2.1	2.4
Anchor design & installation	2.1	2.1	2.0
Advanced tank testing facilities	2.0	2.1	1.7
Wind farm operation (wake effects, yield, AEP)	1.9	2.1	1.0
Advanced modelling tools	1.9	2.5	2.0
High voltage dynamic cables	1.8	2.1	1.6
Bespoke standards for floating wind	1.8	2.0	1.0
Environmental impact	1.4	2.1	1.0

N.B. Scoring from 1-3; High = 3, Med = 2, Low = 1.

Table 1. Prioritisation of key technical barriers for FOWTs, from James and Ros (2015)

Due to their significant cost, the reduction of the size of the platform and the development of new advanced floating platforms is one of the key technical goals James and Ros (2015) of the FOWT industry. Furthermore, improving installation procedures, port-side Operation & Maintenance procedures or developing floating electrical substations, new mooring lines, and anchoring systems are all fields of intense R&D activity. Developing advanced control systems is considered one of the ways to reduce the Levelized Cost of Energy James and Ros (2015). However, estimating the potential savings by adopting advanced control systems is not a simple task. The authors of IRENA (2021) have considered the technological, market and R&D indicators that together can contribute to reducing the LCOE of offshore wind. Developing advanced control systems for offshore wind turbines is directly related to potential cost reductions in several areas:

- increasing Annual Energy Production (AEP) has a direct impact on LCOE
- reducing platform motion helps reduce platform size and weight (platform is the most expensive part of FOWT)

https://doi.org/10.5194/wes-2024-144
Preprint. Discussion started: 21 November 2024

eawe european academy of wind energy
Open Access WIND ENERGY SCIENCE DISCUSSIONS

- reducing vibratory loads on critical components reduces maintenance, increases plant lifetime and helps increase wind turbine size (see Pustina et al. (2021, 2020))

The traditionally adopted control strategy is divided into four operating regions. Region 1 is below the cut-in speed, and the generator is inoperative. Region 2 is between the cut-in speed and the rated wind speed, and the controller tries to maximise the generated power, which is still lower than the rated one. Typically, for large wind turbines, this is achieved by acting on the generator torque to track the optimal tip-speed ratio and setting the collective pitch of the blades at an almost optimal value (constant through the region).

In region 3, above rated wind speed, the controller acts through the collective pitch to keep the rotor angular speed constant (usually via a PI controller), and the generator torque is used to maintain the rated power output.

In the presence of strong winds (region 4), the turbine is turned off to avoid damage. Actual controllers may also include additional transition regimes.

A completely different type of control for wind turbines is Model Predictive Control (MPC). It is based on an optimisation problem that systematically handles blade pitch and generator torque considering nonlinear aerodynamics, constraints on states and inputs (e.g., maximum platform velocities, maximum thrust or power), and complex objective functions. Starting from the updated turbine state, the MPC solves the optimisation problem over a horizon, to find the optimal control law. The evaluated optimal control law is used until the next solution is available from the analysis of the next horizon. The MPC can be formulated to track a reference condition or to maximise or minimise a cost function (e.g., produced energy). In the latter case, in the automatic control field it is commonly refereed as *Economic* NMPC (ENMPC) to highlight that the system trajectory is part of the solution and no predefined reference is used. Recently, the authors developed an ENMPC for maximise power in offshore wind turbines in Pustina et al. (2022a, b). In that work, the reader can find a detailed review of the application of MPC to onshore wind turbines.

For FOWTs, modifications to the standard control laws are necessary due to the absence of a strong constraint on the tower base and the intense action of impinging waves. This is particularly evident in yaw, surge, and sway displacements, which have smaller restoring forces, almost entirely due to the mooring lines' action. The FOWT control is relatively unexplored, but some fundamental issues have been recognised. In control zone 3, for example, lower gains are necessary Jonkman (2010) to reduce the closed-loop rotor natural frequency below the expected sea state frequencies and the natural pitch frequency of the platform. Indeed, in Larsen and Hanson (2007), the authors found this condition ensures positive damping when active pitch-to-feather control is used. However, this reduces the performance of the controller. In addition, the tower bending moments caused by these and inertial/aerodynamic loads may damage the components and structure of the wind turbine. Due to the order of magnitude of these loads, they are difficult to control using the pitch and generator control action. In the future, one can imagine using active mooring systems. Finally, large platform motion (in particular pitch and surge) may reduce/increase power output Fu et al. (2019) and affects the power quality, introducing unwanted harmonics Wen et al. (2018). On the other hand, acting on pitch to control platform motion may also increase power fluctuations Lackner (2009). All this confirms that there is a trade-off between power quality / quantity and platform motion minimisation López-Queija et al. (2022).

https://doi.org/10.5194/wes-2024-144
Preprint. Discussion started: 21 November 2024

eawe european academy of wind energy
Open Access WIND ENERGY SCIENCE DISCUSSIONS

Reference Salic et al. (2019) presents an exhaustive list of control trends in FOWTs. It includes individual pitch control to reduce loads and improve power quality, structural control to minimise loads on the tower/platform system, and multi-objective (power increase and load alleviation) control strategies, including MPC. Some recent examples of MPC applied to FOWTs are present in the literature, covering topics ranging from active mooring systems Wu and Li (2022), to control in the case of pitch actuator failure Thiery et al. (2015), reduction of pitch actuator fatigue Sarkar et al. (2020), and reduction of the motion of the platform, as in Shah et al. (2021) where the authors adopt a linearised reduced order model of an FOWT to build a model prediction controller aimed at reducing the motion of the platform in control region 3, where power regulation is simply a task of tracking the rated value. Similarly, in Jard and Snaiki (2023), the authors have used a linear MPC to track the position of the platform, the speed of the rotor, and the power. Although this is a relevant result, it is far from an actual application of an MPC in FOTWs, since, the power optimization problem is transformed into the tracking of a quasi-steady optimal value of rotor speed, neglecting many dynamic effects. In contrast, this work introduces an Economic NMPC for FOWTs derived from the one presented Pustina et al. (2022a), which may be used in the entire operation range of the turbine. The ENMPC is here extended to multiple objectives, i.e. the reduction of longitudinal platform motion and the increase of power production. To do that, the surge and pitch platform motions (which significantly affect produced power and nacelle motion) are included in the Reduced Order Model used in the ENMPC. The last part of the investigation is devoted to analysing the robustness of ENMPC concerning the prediction of incoming wind and waves. Indeed, ENMPC, as many other control strategies, requires wind prediction Jena and Rajendran (2015). Many approaches have been proposed to this issue. Regarding wind speed estimation, they include LIDAR sensors, upstream meteorological masts, and speed estimations, also using data from upstream turbines of a farm. In Sun et al. (2020), a review of full-scale wind field measurements and the effect of turbine wake on a farm is presented. Concerning waves, the turbine may be equipped with a wave radar Fucile et al. (2016) to estimate the future forces of the sea waves. However, these devices have a non-negligible cost and require maintenance.

The structure of the article is as follows. First, a summary of the novelties is provided. In Section 2 the standard controller is explained being compared with the proposed one. Section 3 initialiy describes the FOWT model and the two Reduced Order Models (ROMs) of the platform. Then the new proposed ENMPC controller is explained with technical details. In Section 4 the ROMs models are validated with OpenFast 1 and the the standard control strategy and the novel controller are compared 2. Finally, the performance of the controller (both in terms of power and platform motion) and its robustness are evaluated by coupling the ENMPC with OpenFAST Jonkman (2013) software on the NREL 5MW turbine Jonkman et al. (2009) supported by a sparbuoy platform Jonkman (2010).

https://doi.org/10.5194/wes-2024-144
Preprint. Discussion started: 21 November 2024

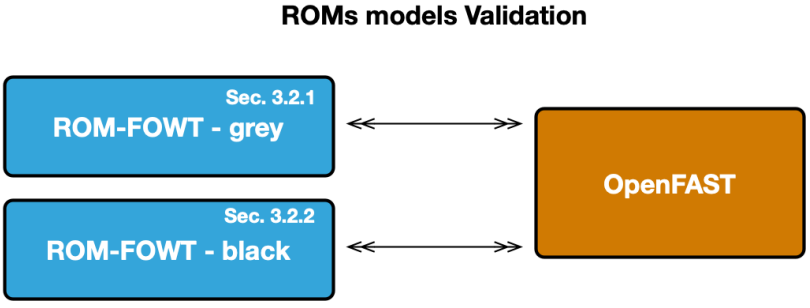

Figure 1. Figure shows that two FOWT with Reduced Order Models, to account for the platform dynamics, have been developed and validated againt the openFAST highly detailed simulation software.

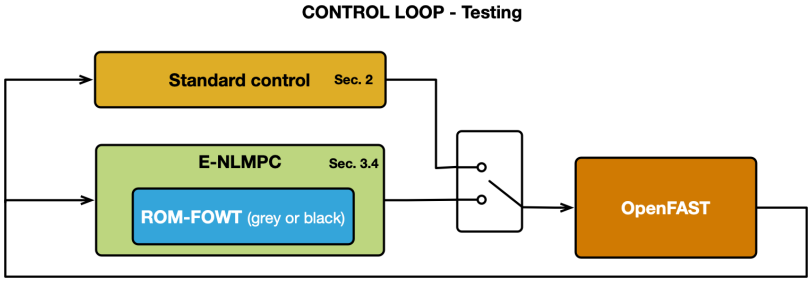

Figure 2. Figure shows that thet standard control strategy and the proposed ENMPC with Reduced Order Models have been used to control a highly detailed FOWT model implemented in openFAST simulation software.

1.1 Improvements with respect to previous works

The following list highlights the novelties of this work in terms of previous works by the authors and in relation to FOWTs:

- a nonlinear equation for dynamic inflow Lydia et al. (2014) and the platform surge and pitch motion equations are added to the rotor model to form a comprehensive reduced-order model of the turbine;
- two different platform models are compared, a grey-box and a black-box model. They consider mooring lines, hydrodynamic, hydrostatic, inertial, and gravitational loads;
- a comprehensive FOWT reduced-order model (ROM) is developed, including platform surge and pitch DoFs;
- the developed ROMs are validated against OpenFAST, the most widely used comprehensive numerical model for wind turbines;
- an ENMPC aimed at power maximisation and reduction of longitudinal platform motion is developed for the whole operating range;

https://doi.org/10.5194/wes-2024-144
Preprint. Discussion started: 21 November 2024

eawe european academy of wind energy
Open Access WIND ENERGY SCIENCE DISCUSSIONS

- a multiobjective analysis is carried out to find the best trade between power maximisation and load reduction.
- The control strategy is solved efficiently in real time with an indirect approach (see section 3.4). Almost any other MPC and NMPC-based approach is based on direct methods, which have been demonstrated to be numerically less efficient and unsuitable for real-time applications Lio et al. (2014). The performance improvement obtained with a non-uniform time mesh is assessed;
- the controller performances are assessed with realistic high-fidelity simulations considering a broad set of sea and wind conditions. This has not been done to this extent in the articles available in the literature;

2 Standard control strategy for FOWTs

Typically, wind turbine controllers aim to maximise power production in operating region 2 (below the rated wind speed) and limit rotor speed and power production in region 3 (above the rated wind speed).

In region 2, the controller allows the wind turbine to operate at the maximum power coefficient $C_P(\lambda, \beta)$. This is usually achieved by fixing the collective pitch to an optimal value (β_{opt}) and acting on the generator torque to maintain the optimal tip speed ratio (λ_{opt}).

Neglecting friction torque, for a steady condition, the aerodynamic torque is equal to the generator one Burton et al. (2011), namely

$$J_{rot}\dot{\Omega} = 0 = \frac{\rho\pi R^2 V_w^3 C_P(\lambda_{opt}, \beta_{opt})}{2\Omega} - \tau_{gen} \tag{1}$$

Multiplying and dividing by λ_{opt}^3, one can obtains:

$$\tau_{gen} = \frac{\rho\pi R^5 C_P(\lambda_{opt}, \beta_{opt})}{2\lambda_{opt}^3}\Omega^2 = k_T\Omega^2 \tag{2}$$

Since K_T does not depend on wind speed, the controller implementation is straightforward.

Floating wind turbines requires different controllers than fixed ones (for a complete review on this topic, refer to López-Queija et al. (2022). In particular, as stated in the introduction, in region 3, the control must differ with respect to onshore turbines to ensure pitch and surge motion damping. In the onshore case, the blade (collective) pitch is modified through a PI controller (see Ref. Jonkman et al. (2009)) to reject disturbances in the rotor speed with respect to the rated value. The generator power is kept constant, slightly modifying the torque according to the rotor speed. Unfortunately, low-damped pitch and surge motion typically occur if the same controller is used on a FOWT, due to the adverse interaction of the controller with the platform pitch motion, which has a significantly lower frequency with respect to that of the fore-aft tower bending mode of an onshore WT. This is because, when the relative wind speed increases due to a forward motion of the nacelle, the PI controller acts to reduce the blade angle of attack, also reducing thrust. This causes a further forward acceleration of the turbine. This phenomenon has been confirmed in Yang et al. (2023), where a detailed analysis of the aerodynamic damping of a semi-submersible floating wind turbine has been carried out. In that case, in region 3, the reduction in pitch motion damping has been found to reach

https://doi.org/10.5194/wes-2024-144
Preprint. Discussion started: 21 November 2024

eawe european academy of wind energy
Open Access WIND ENERGY SCIENCE DISCUSSIONS

80 %. In addition to lower controller gains (to have a rotor closed-loop frequency below the typical sea-state frequency and a natural pitch frequency of the platform Jonkman (2010)), a constant generator torque is usually adopted in operating region 3 to further increase closed-loop damping of the rotor. Note that, by using a constant generator torque, fluctuations of the generated power arise due to the difficulty of precisely controlling in rotor speed due to its large inertia, thus inducing a poorer power quality. In the literature, other control strategies have been proposed to avoid this problem. In some cases (e.g. Fleming et al. (2014)), the constant detuning strategy explained above has been modified to scheduled detuning, varying the gains with wind speed. In many other cases (e.g. Yu et al. (2018) the control strategy included some additional input into the pitch or torque controller, typically pitch angular velocity or nacelle velocity. Other different controllers based on different theories have also been proposed, such as the application of H_∞ control theory Hara et al. (2017), LQR Bagherieh and Nagamune (2015), or adaptive super-twisting control Zhang and Plestan (2020). In other cases, the collective control strategy has been abandoned in favour of individual blade control (e.g. Namik and Stol (2013)).

This work uses the controller described in Jonkman et al. (2009) with modified gains and a constant torque strategy in region 3 as a reference controller.

3 Reduced order models for floating offshore wind turbines

To develop a real-time model predictive controller, it is crucial to utilise a computationally efficient Reduced Order Model (ROM) that captures the essential system dynamics. This section presents a new ROM specifically developed for floating wind turbines, which incorporates both the rotor's low-frequency dynamics and the platform's primary dynamics. Validation of the ROM against the OpenFAST model (see section 4.2) ensures an accurate estimation of the key dynamics of the system. Subsequently, the ROM is integrated into the model predictive controller and is evaluated in closed-loop simulations with OpenFAST, comparing its performance with traditional control strategies.

section 3.4).

The complete FOWT ROM is given by the combination of a nonlinear ROM describing rotor aeromechanics (see section 3.1) and a single-node equation for thermal dynamics estimation (following what the authors proposed in Pustina et al. (2022a)) with a linear ROM for the description of platform dynamics (see section 3.2.1 and section 3.2.2).

Platform motions, notably surge and pitch (the two degrees of freedom considered in this work, see fig. 3), affect the velocity of the hub and rotor blade. As will be shown in the next section, the other platform DoFs (sway, heave, roll, and yaw) have a limited impact on aerodynamics since they slightly modify the velocity perpendicular to the rotor. The aerodynamic power depends on the third power and the thrust on the second power of the relative wind speed. Therefore, it is paramount to consider the motion of the platform when developing a ROM for FOWTs. Furthermore, as for standard controllers, an offshore controller is likely to make the FOWT dynamically unstable (see section 2) and must be sufficiently modified Jonkman (2010). A reliable estimation of the motion of the platform is then required to define an effective and robust ENMPC for FOWT, which includes the motion of the platform as a constraint or its minimisation as part of the objective. In this work, a rotor ROM based on unsteady wake inflow (see the next section) is coupled with a two-degree-of-freedom platform model, forced by wave loads

https://doi.org/10.5194/wes-2024-144
Preprint. Discussion started: 21 November 2024

eawe european academy of wind energy
Open Access WIND ENERGY SCIENCE DISCUSSIONS

and rotor thrust. The coupling with the wind turbine model is obtained in terms of thrust and pitching moment transmitted by the tower to the platform and, vice versa, through the kinematics imposed by the platform to the tower.

Two approaches are proposed to model the platform dynamics: 1. a grey-box approach where part of the system is described using known properties of the system (e.g. the mass properties) and the other forces are singularly analytically expressed or identified from simulations (see section 3.2.1); 2. a linear black-box ROM completely identified from high-fidelity simulations outputs (see section 3.2.2), where all the forces acting on the platform are considered as a whole.

All proposed ROMs are validated against OpenFAST simulations (see section 4.2) .

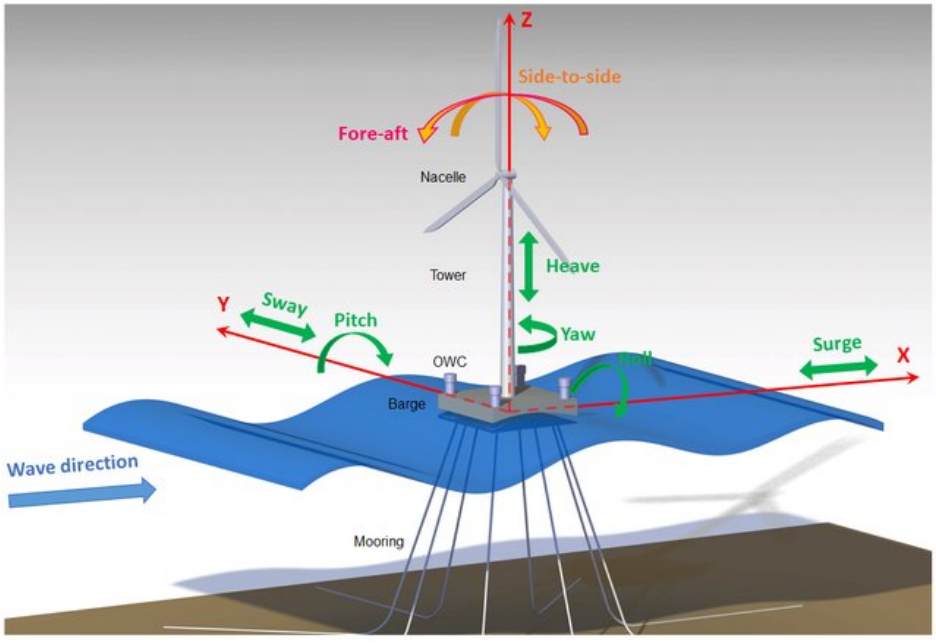

Figure 3. Floating Offshore Wind Turbine with reference frame description. Source:Aboutalebi et al. (2021)

3.1 Rotor dynamics with dynamic wake inflow and platform motion effects

Typically, a nonlinear, one-DoF turbine model with steady aerodynamics is used for control synthesis purposes Henriksen et al. (2011); Yan et al. (2013), namely

$$J_{rot}\dot{\Omega} = \tau_{aero} - \tau_{gen} \tag{3}$$

where J_{rot} is the turbine equivalent inertia (relative to low-speed shaft angular velocity Ω), τ_{aero} the aerodynamic torque, and τ_{gen} the generator torque (multiplied by the gearing ratio). The aerodynamic torque can be expressed as:

$$\tau_{aero} = \frac{P_{aero}}{\Omega} = \frac{\rho \pi R^2 V_w^3 C_P}{2\Omega} \tag{4}$$

where P_{aero} is the aerodynamic power, R represent the rotor radius, V_w is the wind speed, and C_P denotes the power coefficient.

https://doi.org/10.5194/wes-2024-144
Preprint. Discussion started: 21 November 2024

eawe european academy of wind energy
Open Access WIND ENERGY SCIENCE DISCUSSIONS

This rotor ROM is based on steady aerodynamics and is accurate in case of steady conditions. The model's accuracy is reduced in the presence of nonuniform winds or, more generally, when unstable aerodynamic conditions provide significant contributions to the loads.

Following Pustina et al. (2022a), the vorticity evolution effects are included via the widely-used nonlinear dynamic inflow Leishman (2016), derived from the Pitt-Peters model Pitt and Peters (1981).

In addition, when the rotor dynamics model is part of a comprehensive solver for FOWTs dynamics simulation, it has to consider the kinematics due to platform motion. The two platform degrees of freedom that mainly affect turbine aerodynamics are surge (σ) and pitch (γ) motion. Indeed, the surge motion induces a uniform velocity distribution, whereas the pitch motion induces a linearly varying velocity distribution, both approximately orthogonal to the disk. Although a detailed description of the effects of platform motion on rotor aerodynamics involves complex phenomena Dong and Viré (2022), to roughly include these effects in the rotor dynamics model, the resulting horizontal velocity of the nacelle, V_{nac}, is introduced to correct for the definition of the mean relative velocity between air and rotor. Indeed, the horizontal nacelle velocity can be easily defined considering the surge velocity, $\dot{\sigma}$, and the pitch angular velocity, $\dot{\gamma}$:

$$V_{nac} = \dot{\sigma} + \dot{\gamma} z_{hub} \tag{5}$$

where z_{hub} is the hub height.

Thus, considering the nacelle velocity influence, the rotor ROM reads:

$$\begin{cases} J_{rot}\dot{\Omega} = \dfrac{1}{2\Omega}\rho\pi R^2 (V_w - V_\lambda - V_{nac})^3 C_P^u - \tau_{gen} \\ m_a \dot{V}_\lambda = -2\rho\pi R^2 V_\lambda (V_w - V_\lambda - V_{nac}) + \dfrac{1}{2}\rho\pi R^2 (V_w - V_\lambda - V_{nac})^2 C_T^u \end{cases} \tag{6}$$

where $m_a = 0.637\rho(4\pi R^3/3)$ denotes the apparent aerodynamic mass, V_λ is the mean wake inflow, C_T^u and C_P^u represent the coefficients of unsteady aerodynamic thrust and power. The influence of relative effective velocity $(V_w - V_\lambda - V_{nac})$ on thrust T^u and aerodynamic power P_{aero}^u is taken into account by modifying the expressions relating power and thrust to their nondimensional coefficient. The same strategy for determining C_P^u and C_T^u described in Pustina et al. (2022a) is used. The coefficients are evaluated considering the aerodynamics of a sequence of steady operating conditions of the isolated rotor. Thus, the same C_P^u and C_T^u of the onshore case are adopted (see Pustina et al. (2022a)). A Radial Basis Functions interpolator is used to derive an analytical expression of the thrust and power coefficients as a function of (Ω, V_w, β) as explained in Pustina et al. (2022a).

3.2 Platform dynamics

As stated before, the surge and pitch model is implemented in the turbine ROM to estimate FOWT motion sufficiently (at least for power production purposes). The platform is dynamically forced by its own weight, the rotor/tower complex, the hydrodynamic/hydrostatic loads, and the mooring lines load.

https://doi.org/10.5194/wes-2024-144
Preprint. Discussion started: 21 November 2024

eawe european academy of wind energy
Open Access WIND ENERGY SCIENCE DISCUSSIONS

Hydrodynamic loads may be divided into diffraction, radiation, and viscous loads. As in the standard linear model, the diffraction loads do not depend on the motions of the platform and provide an exogenous forcing term to the model. The second type of exogenous forcing terms in the platform model is that transmitted by the tower.

Two approaches can be followed to build the platform ROM as part of the comprehensive FOWT model. A first grey-box model is derived by coupling the platform rigid body motion equations with the loads transmitted by the tower, the water loads and the mooring lines loads, singularly modelled. The alternative black-box model relies on the numerical identification of a ROM of a linear platform based on a set of simulations provided by the OpenFAST high-fidelity solver (see section 3.2.2). In the latter case, the FOWT model is derived by coupling the platform ROM only with generic exogenous forcing terms (because the platform ROM implicitly considers mooring lines and radiation forces).

3.2.1 Grey-box ROM for platform dynamics

The grey-box model is represented in the following form:

$$\mathbf{M}_{ine}\ddot{\mathbf{q}} = \mathbf{f}_{ml} + \mathbf{f}_{rad} + \mathbf{f}_{hyst} + \mathbf{f}_{visc} + \mathbf{f}_{diff} + \mathbf{f}_{rot} \tag{7}$$

where $\mathbf{q}$ collects surge and pitch platform DoFs, $\mathbf{M}_{ine}$ is the inertial matrix, whereas $\mathbf{f}_{ml}$, $\mathbf{f}_{rad}$, $\mathbf{f}_{hyst}$, $\mathbf{f}_{diff}$, $\mathbf{f}_{rot}$ denote the loads given by, respectively, mooring lines, hydrodynamic radiation, hydrostatics, hydrodynamic diffraction and tower/rotor complex. The latter contribution is limited to the thrust assumed to be applied at the centre of the hub. A simple expression of the hydrodynamic forces and moments is necessary to maintain the ROM suitable for real-time control applications. A first-order linear model is used for the hydrostatic loads, namely $\mathbf{f}_{hyst} = \mathbf{K}_{hyst}\mathbf{q}$, which depend only on the effect of the pitch on the immersed volume of the platform. The memory effects of the hydrodynamic loads (related to free-surface deformation) are not considered to reduce the model order. Only the added mass related to the hydrodynamic radiation loads is considered, that is, $\mathbf{f}_{rad} = \mathbf{M}_{rad}\ddot{\mathbf{q}}$.

In eq. (7), the term $\mathbf{f}_{visc}$ introduces a linear damping term that cannot be neglected in the evaluation of hydrodynamic damping. These additional damping loads are related to surge and pitch velocity by the following expression $\mathbf{f}_{visc} = \mathbf{C}_{visc}\dot{\mathbf{q}}$. Following Jonkman (2010), the coefficients are determined by matching the measured free-decay response in still water.

The force of the anchor lines $\mathbf{f}_{ml}$, which act on the platform, is modelled through a transfer function $\mathbf{H}_{ml}(s)$ (namely, such that $\tilde{\mathbf{f}}_{ml} = \mathbf{H}_{ml}\,\tilde{\mathbf{q}}$). The transfer function is identified with the MoorDyn tool Hall (2015) from dynamic responses to perturbations of the platform motion.

Then, following Gennaretti et al. (2017), the transfer matrix may be approximated in rational-matrix form. However, a preliminary analysis has shown that no relevant poles are present in the frequency range of interest, and hence the transfer functions may be approximated as

$$\mathbf{H}_{ml}(s) \approx s^2\mathbf{M}_{ml} + s\mathbf{C}_{ml} + \mathbf{K}_{ml} \tag{8}$$

thus yielding

$$\mathbf{f}_{ml}(t) \approx \mathbf{M}_{ml}\ddot{\mathbf{q}} + \mathbf{C}_{ml}\dot{\mathbf{q}} + \mathbf{K}_{ml}\mathbf{q} \tag{9}$$

https://doi.org/10.5194/wes-2024-144
Preprint. Discussion started: 21 November 2024

It should be noted that the spring matrix $\mathbf{K}_{ml}$ is determined from steady responses since there are no poles. In contrast, the mass and damping matrices, $\mathbf{M}_{ml}$ and $\mathbf{C}_{ml}$, are determined from responses to high-frequency platform motions, the former as the quadratic coefficient that fits the real part of the transfer function, and the latter as the linear coefficient fitting the imaginary part of it. Moreover, since preliminary analyses have shown that $\mathbf{M}_{ml}$ is negligible with respect to the inertial matrix of the platform, it has been neglected.

3.2.2 Black-box ROM for platform dynamics

A second possibility of building the ROM of the platform is the black-box approach, where high-fidelity simulations performed with OpenFAST are used directly to identify the model. The inputs of the platform ROM, collected in the vector $\mathbf{u}$, are the aerodynamic thrust applied at the centre of the hub and the diffraction forces, whereas the outputs, collected in $\mathbf{y}$, are surge and pitch displacements and velocities of the platform.

The Matlab VV.AA. (2019a) function *n4sid* Van Overschee and De Moor (2012); Verhaegen (1994) is used to identify a linear state-space model, namely

$$\begin{aligned} \dot{\mathbf{x}} &= \mathbf{A}\,\mathbf{x} + \mathbf{B}\,\mathbf{u} \\ \mathbf{y} &= \mathbf{C}\,\mathbf{x} \end{aligned} \tag{10}$$

The vector $\mathbf{x}$ collects the states of the ROM. They are not the whole set of model DoFs, but rather the states more relevant for the transfer functions relating inputs and outputs of interest. For platforms on which the hydrodynamic radiation memory effect is more relevant, the states would also include hydrodynamic ones. In the spar buoy case (where the radiation memory effect can be neglected), the states have been chosen in the same number as the outputs (four). In this case, $\mathbf{C}$ is a square matrix that can be inverted.

The identified state-space can be rewritten as:

$$\dot{\mathbf{y}} = \mathbf{C}\mathbf{A}\mathbf{C}^{-1}\,\mathbf{y} + \mathbf{C}\mathbf{B}\,\mathbf{u} \tag{11}$$

In this form, the states and the outputs coincide, and they have an easily recognisable physical meaning.

In this work, both the comprehensive FOWT platform ROMs are validated in section 4.2. The black-box approach presents several advantages:

- it is simpler to develop
- it can also be built using experimental data without the need for a high-fidelity solver (platform motions and rotor thrust can be measured, and diffraction forces can be estimated numerically)
- is more suited for multibody platforms concepts like Tetraspar or Hexafloat models Borg et al. (2020).

In contrast, a grey-box model has the advantage of being modular, so it allows the evaluation of the effect of changing a component or its modelling fidelity and rapidly evaluating the effect on the system dynamics.

https://doi.org/10.5194/wes-2024-144
Preprint. Discussion started: 21 November 2024

eawe european academy of wind energy
Open Access WIND ENERGY SCIENCE DISCUSSIONS

3.3 Simplified generator thermal model

Different from standard control strategies presented in the literature, a single-node generator temperature model is included in this work as in Pustina et al. (2022a). This is to take into account the large thermal capacity of the generator that allows overriding the rated power for a considerable time, increasing power production and avoiding generator damage. The same thermal model developed in Pustina et al. (2022a) is used here.

3.4 Proposed Non-Linear Reciding Horizon Control

This work applies an Economic Non-linear Model Predictive Controller (ENMPC) to maximise power production and reduce longitudinal platform motions. Unlike standard control techniques (see section 2), this approach can be applied in the entire FOWT functioning range, without the need to define different control laws, thanks to the ability to handle user-defined objective functions and constraints. The ENMPC defines a sequence of control actions by solving optimisation problems over overlapping finite time intervals. The optimal problem is subject to several constraints to avoid generator overheating, wind turbine overloading, and unacceptable platform motion (to prevent overloading on mooring lines and electric cables).
To avoid the tendency to slow down the rotor in the final part of each time horizon to increase the generated power (see Pustina et al. (2022a)), the power maximisation objective is expressed in terms of aerodynamic power

$$J_{pow} = \int_{T_0}^{T_0+T_w} -P_{aer}\ \mathrm{d}t \tag{12}$$

where T_0 is the actual time instant and T_w is the optimisation time horizon. In addition, a term that depends on the longitudinal nacelle velocity is added to reduce longitudinal platform motions. Thus, the scaled and weighted sum of the expression of the integral cost function is:

$$J = \int_{T_0}^{T_0+T_w} -\left((1-w)\frac{P_{aer}}{P_{rat}} - w\frac{V_{nac}^2}{V_{ref}^2}\right)\ \mathrm{d}t \tag{13}$$

where P_{rat} is the rated power, $w \in [0,1]$ is the relative weight of the nacelle velocity term and V_{ref} is a reference nacelle velocity. This work considers $V_{ref} = 0.5$ m/s, a typical standard deviation for the load cases considered.

https://doi.org/10.5194/wes-2024-144
Preprint. Discussion started: 21 November 2024

eawe european academy of wind energy
Open Access WIND ENERGY SCIENCE DISCUSSIONS

The selected constraints for the optimal control problem are:

$$\beta_{min} < \beta < \beta_{max} \tag{14a}$$

$$\tau_{min} < \tau < \tau_{max} \tag{14b}$$

$$\dot{\beta} < \dot{\beta}_{max} \tag{14c}$$

$$\dot{\tau} < \dot{\tau}_{max} \tag{14d}$$

$$\omega < \omega_{max} \tag{14e}$$

$$\theta < \theta_{max} \tag{14f}$$

$$P^{gen} < P^{gen}_{max} \tag{14g}$$

$$T < T_{max} \tag{14h}$$

$$\dot{\sigma} < \dot{\sigma}_{max} \tag{14i}$$

$$\dot{\gamma} < \dot{\gamma}_{max} \tag{14j}$$

and must be interpreted as:

- the pitch β is limited to avoid stall (see eq. (14a));
- the generator torque τ is constrained to avoid excessive overcharging on the generator (see eq. (14b));
- the pitch rate $\dot{\beta}$ and the torque rate $\dot{\tau}$ are constrained accordingly to actuation system specifications (see eq. (14c) and eq. (14d));
- the rotor speed Ω is limited by the maximum tip-speed eq. (14e)
- the generator temperature θ is limited to avoid damages (see eq. (14f);
- the instantaneous generated power P^{gen} (+20% the rated value) is limited since power electronics have very limited capacity to override nominal conditions (see eq. (14g)). Note that, also in the standard offshore controller case, the power electronics must be up-sized. Indeed, the standard offshore controller in operating region 3 has low proportional and integral gains and adopts a constant torque strategy (see section 2) increasing the power oscillations with respect to the onshore controller.
- thrust is constrained to avoid bearings and tower overloading eq. (14h);
- constraints eq. (14i) and eq. (14j) respectively on the maximum surge velocity, $\dot{\sigma}$, and the maximum platform pitch velocity, $\dot{\gamma}$, are included in order to ensure stable platform dynamics and limited platform motions (thus avoiding high stresses on mooring lines and electric cable). These limits are set according to the maximum values obtained with the reference controller.

https://doi.org/10.5194/wes-2024-144
Preprint. Discussion started: 21 November 2024

eawe european academy of wind energy
Open Access WIND ENERGY SCIENCE DISCUSSIONS

In receding-horizon controllers, as here implemented, it is important to ensure the continuity of the control variables and also of their time derivative in order that the sequence of optimised control actions over the horizon T_w is smooth. Therefore, the nonlinear FOWT ROM of section 3 is augmented with the following equations:

$$\dot{\tau} = v_\tau \tag{15a}$$

$$\dot{\beta} = v_\beta \tag{15b}$$

$$\dot{v_\tau} = a_\tau \tag{15c}$$

$$\dot{v_\beta} = a_\beta \tag{15d}$$

where v_β and a_β are the blade pitch angular velocity and acceleration, v_τ and a_τ are the generator torque first and second time derivative. With the above, the general NMPC scheme over the horizon T_w adopted here reads:

$$\text{minimize}: \quad J(\mathbf{x},\mathbf{u}) = \int_{T_0}^{T_0+T_w} -\left((1-w)\frac{P_{aer}}{P_{rat}} - w\frac{V_{nac}^2}{V_{ref}^2}\right) \mathrm{d}t \tag{16a}$$

$$\text{subject to}: \quad \dot{\mathbf{x}} = \mathbf{f}(\mathbf{x},\mathbf{u}) \tag{16b}$$

$$\mathbf{x}(t_0) = \mathbf{x}_0 \tag{16c}$$

$$\mathbf{c}(\mathbf{x}) \geq \mathbf{0} \tag{16d}$$

where eq. (16d) is the list of constraints defined in eq. (14), eq. (16b) contains the equations of the FOWT ROM described in section 3 enriched by the assumption in eq. (15), $\mathbf{x}^T = \{\Omega, \lambda, \sigma, \dot{\sigma}, \gamma, \dot{\gamma}, \theta, \tau, \beta, v_\tau, v_\beta\}$ is the list of states and $\mathbf{u}^T = \{a_\tau, a_\beta\}$ is the vector of the controls.

The derivative of $\{v_\tau$ and $v_\beta\}$ become states of the augmented ROM. At each new control law computation, the initial values of these new states are imposed according to the last control window to have a C1 continuity.

The same approach for the numerical solution of the Optimal Control Problem used in Pustina et al. (2022a) is adopted here. It is based on an indirect method related to the Pontryagin Minimum Principle Pontryagin (1987) to derive the necessary conditions of optimality Liberzon (2011), and it is implemented in the PINS code Biral et al. (2016), developed by Trento University and freely available for academic use (contact the authors).

The combination of the non-linearity of the system dynamics and of the inequality constraints poses some difficulties in reaching the solution convergence in the real-time application. The issue is compounded by the mismatch between the model used in the ENMPC formulation and the actual dynamics, which could result in initial conditions, estimated from the actual system state, very close to the limits or even over the limits (e.g. the rotor thrust). Therefore, a number of remedial strategies can be implemented to improve the convergence rate and meet the application control frame rate, namely *shift initialisation*, *homotopy* and *constraint violation relaxation*.

https://doi.org/10.5194/wes-2024-144
Preprint. Discussion started: 21 November 2024

eawe european academy of wind energy
Open Access WIND ENERGY SCIENCE DISCUSSIONS

3.4.1 Shift initialisation

In order to warm start, the solver part of the previous step solution is used to initialise the new problem. It is motivated by the principle of optimality of sub-arcs Gros and Diehl (2022). With a moving horizon, the first part of the solution is cut and the end is prolonged (see Figure 4). If the re-planning is done frequently and the dynamic model is sufficiently accurate, the part that is kept is expected to be not far from the optimal solution provided that perturbations are limited and the new initial states estimate are not too far from real $\mathbf{x}_0(t_{k+1})$.

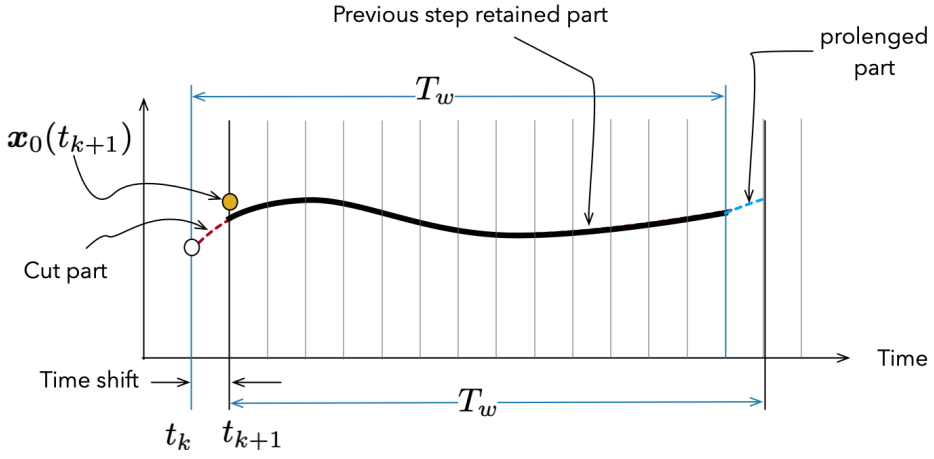

Figure 4. Visualisation of the time shift concept. Figure4 shows the retained part of the previous step solution, the cut and prolonged parts, and the estimated initial states that might not coincide with the initial state predicted by the previous solution.

3.4.2 Homotopy

The basic idea is to solve a series of neighbouring optimization problems that progressively approximate the original problem. In particular, PINS handles the inequality equations of the form $c(\mathbf{x}) \geq 0$ (but it can manage more general inequalities of the form $a \leq c(\mathbf{x}, \mathbf{u}, t) \leq b$) that are approximated with penalty functions:

$$c(\mathbf{x}) \geq 0 \approx \text{TARGET} \oplus \int_{T_0}^{T_0+T_w} \mathcal{P}(c(\mathbf{x}), \epsilon, h)\mathrm{d}t \tag{17}$$

The parameters ϵ and h control the penalty function curve, and in particular, for ϵ and $h \to 0$, the penalty approximates the exact inequality (see left Figure 5).

https://doi.org/10.5194/wes-2024-144
Preprint. Discussion started: 21 November 2024

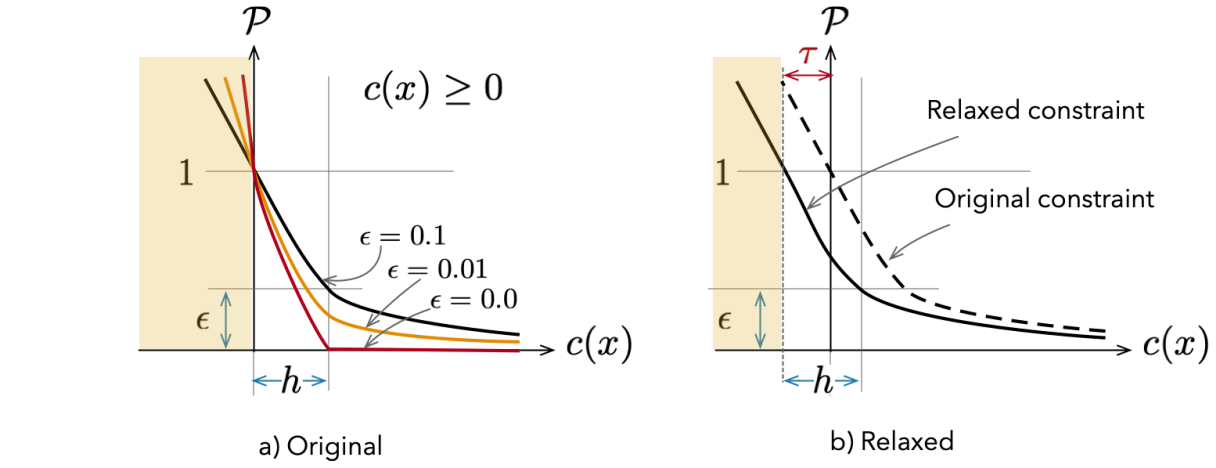

Figure 5. Penalty function $\mathcal{P}(c(x), \epsilon, h)$ for decreasing values of ϵ. On the left, it is shown the homotopy process with the effect of decreasing the parameter ϵ. On the right, the relaxation concept is explained: the constraint is moved by an amount τ in order to let the initial conditions satisfy the constraints.

The use of a penalty function instead of a barrier has the advantage of allowing the argument $c(x)$ of the inequality to violate the constraint during the iteration to convergence. In contrast, when the parameter ϵ goes to zero, the gradient of the penalty close to the limit becomes extremely large, jeopardising the convergence rate. Therefore, to facilitate convergence, the initial value of the parameter ϵ is large (approximately 0.1). Then it is progressively decremented each time a new optimisation problem is solved using the previous step solution as a guess. The process is stopped when the minimum value for the parameter ϵ is reached that is small enough to approximate the original inequality constraint. A draft of the homotopy strategy is given in 1. One may note that since at each homotopy iteration, the solver must find a solution to proceed with a new value of parameter ϵ, in case it does not converge, an intermediate solution can be used as a suboptimal solution.

3.4.3 Constraint violation relaxation

The third mechanism implemented to improve the convergence rate has to deal with initial conditions that do not satisfy constraint equations. It may be possible that, due to the inaccuracies of the adopted dynamic model and/or the effect of external perturbations, the real system deviates from the predicted behaviour. Thus, the new initial conditions ($x0(t_{k+1})$ in Figure4) may not satisfy the inequality constraints. In this case, it is possible to locally (that is, in the first part of the planning horizon) relax the constraint equations moving the limit of a quantity $\tau(t)$ modifying the inequality constraint into $c(x) + \tau(t) \geq 0$. The parameter $\tau(t)$ can be a constant parameter or a function of time. In the latter case, $\tau(t)$ can be decreased along the planning horizon to force the solution back into the feasible region (i.e., satisfy the inequality constraints).

https://doi.org/10.5194/wes-2024-144
Preprint. Discussion started: 21 November 2024

eawe european academy of wind energy
Open Access WIND ENERGY SCIENCE DISCUSSIONS

Algorithm 1 Homotopy for penalties for s different homotopy strategy steps

Initialize $\epsilon_k \leftarrow \epsilon_{k,\max}$ and $h_k \leftarrow h_{k,\max}$ with $k = 1, 2, \ldots, p$ for all the p penalties
Solve the nonlinear system (representing the approximation of the OCP problem)
for $m = 1, 2, \ldots, N$ **do**
    Start the n-th homotopy stage of the N total
    $s \leftarrow 0$; $\Delta s \leftarrow c_0$ {Constant satisfy $c_0 \in (0, 1)$ for example $c_0 = 0.1$}
    while $s < 1$ **do**
        Save $s_{\text{old}} \leftarrow s$
        Update $s \leftarrow s + \Delta s$ and update the group of penalties of the m-th homotopy
        with the rule $\epsilon_k \leftarrow (1 - s)\epsilon_{k,\max} + s\epsilon_{k,\min}$ and $h_k \leftarrow (1 - s)h_{k,\max} + sh_{k,\min}$
        Solve the nonlinear system with the updated parameters and guess the last computed solution.
        if converged? **then**
            if used few iterations? **then**
                Increase $\Delta s \leftarrow c_1 \Delta s$; {Constant satisfy $c_1 > 1$ for example $c_1 = 1.5$}
            end if
            Save computed solution
        else
            if $\Delta s < \Delta s_{\min}$ **then**
                Homotopy failed, return last computed solution
            end if
            Convergence failed, reset to last saved computed solution and reset $s \leftarrow s_{\text{old}}$
            Reduce $\Delta s \leftarrow c_2 \Delta s$ {Constant satisfy $c_2 \in (0, 1)$ for example $c_2 = 0.5$}
        end if
    end while
end for

4 Results and discussion

The numerical results are organised as follows. First, the developed ROMs are validated with high-fidelity simulations, and their ability to predict the evolution of the wind turbine using a reference controller is evaluated. Then, the performance of the proposed ENMPC is assessed on a realistic set of cases of wind and sea state closing the loop on the FOWT simulator. The analysis considers typical sea states and wind velocities of a deep-water site in the Dutch North Sea (see Fischer et al. (2010)). The significant wave height, the peak-spectral wave period and the mean wind speed of the considered Load Cases (LCs) are reported in table 2.

https://doi.org/10.5194/wes-2024-144
Preprint. Discussion started: 21 November 2024

eawe european academy of wind energy
Open Access WIND ENERGY SCIENCE DISCUSSIONS

Load case	Mean wind speed [m/s]	Significant wave height [m]	Peak-spectral wave period [s]
LC1	4	1.96	9.72
LC2	6	2.23	9.77
LC3	8	2.53	9.85
LC4	10	2.85	9.97
LC5	11	3.02	10.04
LC6	12	3.20	10.11
LC7	13	3.38	10.19
LC8	14	3.58	10.27
LC9	16	3.97	10.44
LC10	18	4.38	10.63
LC11	20	4.80	10.82
LC12	22	5.24	11.02
LC13	24	5.69	11.23

Table 2. Load cases main parameters.

All LCs are imposed according to the IEC 61400-3 standard VV.AA. (2006). In detail, the IEC Kaimal spectral model, the standard IEC C category of turbulence, and the power-law mean wind profile Jonkman and Buhl Jr (2006) (with a reference height of 90 m and a power coefficient equal to 0.14 are considered). The sea states are multidirectional, short-crested, and characterised by a JONSWAP spectrum Hasselmann et al. (1973), with significant wave heights and peak wave periods reported in table 2. A cosine spreading function is used to define the directional spreading spectrum Duarte et al. (2014).

Considering the wide set of LCs reported in table 2, the ENMPC is tested in the entire operating regions 2 and 3. First, the proposed single-objective ENMPC is compared with the reference and the ENMPC controller for onshore turbines developed in Pustina et al. (2022a). Then, the multi-objective ENMPC performance is analysed: the Pareto front for $LC6$ is used to choose the best relative weight, and the controller is compared against the reference and the single-objective for all LCs.

Finally, considering the difficulty in predicting the sea diffraction forces and the incoming wind, the multi-objective ENMPC performance is assessed in the absence of this information.

4.1 Simulator of platform and wind turbine models

In this work, the numerical test case is the widely used NREL-5MW Jonkman et al. (2009) supported by the spar-buoy OC3 platform Jonkman (2010). This combination of turbine and platform is relatively more prone to large platform motions. In fact, in Pustina et al. (2023), the authors have tested controllers for minimise sea-induced loads in three different FOWT: the NREL-5MW Jonkman et al. (2009) supported by the spar-buoy Jonkman (2010), the NREL-5MW supported by the semi-sub platform

https://doi.org/10.5194/wes-2024-144
Preprint. Discussion started: 21 November 2024

defined in Robertson et al. (2014), and the IEA 15MW Gaertner et al. (2020) wind turbine supported by the UMaine VolturnUS-S semi-sub platform Allen et al. (2020). The NREL-5MW/OC3 was the most critical FOWT for the offshore controller due to its lower restoring forces. Although future larger FOWTs will be inherently less prone to large motion, reducing the size of the platform and the overall weight of the turbine is a way to reduce capital costs. Thus, the ability to control the motion will also be an interesting feature for future turbines.

Open-source software OpenFAST software Jonkman (2013) is used to simulate the dynamic response of high-fidelity wind turbines. The model includes the complete motion of the platform and approximates the tower elasticity with four modes, and the blade elasticity with three modes (two flap modes and one lead-lag mode).

Wake inflow is estimated using the Generalised Dynamic Wave (GDW) model Moriarty and Hansen (2005) which includes tip losses, hub losses, and skewed wake effects. The Beddoes-Leishman dynamic stall formulation is used for the evaluation of aerodynamic loads Moriarty and Hansen (2005). The thermal model described in section 3.3 is also implemented in OpenFAST.

4.2 Validation of the developed FOWT ROMs

As described in section 3, the black and grey-box platform ROMs are coupled with the nonlinear rotor ROM in a comprehensive FOWT ROM, the platform being forced by the rotor thrust, and the platform motion altering rotor kinematics. In Pustina et al. (2022a), the authors have tested and compared several rotor ROMs. For an onshore configuration, it has been shown that the rotor ROM with the inclusion of wake inflow and using three-variable aerodynamic coefficient maps is more accurate than those available in the literature Henriksen et al. (2011); Yan et al. (2013); Schlipf et al. (2013).

The comprehensive FOWT ROMs using the grey-box and black-box platform models are validated and compared here. They are also compared with the rotor ROM without the nacelle velocity contribution to highlight the effect of the platform motion on the rotor aerodynamics. The reference controller Jonkman et al. (2009); Jonkman (2010), which requires only in measuring rotor speed, is straightforwardly coupled to the ROM. In contrast, the rotor ROM requires the instantaneous value of the effective wind speed over the entire disc, here approximated with the mean axial wind speed over the disc. Moreover, the surge and pitch diffraction forces acting on the platform in OpenFAST are considered to be forcing inputs for the FOWT ROMs.

Figure 6 depicts the root mean square error (RMSE) in aerodynamic thrust and power as evaluated by the ROMs and OpenFAST for all LCs considered. The 'onshore' rotor ROM does not include platform motions. The black-box and grey-box floating ROMs include the aerodynamic correction due to the longitudinal nacelle velocity and the platform dynamics. As expected, the accuracy of the two FOWT ROMs is higher with respect to the onshore ROM, since the nacelle velocity is not negligible with respect to wind velocity. Obviously, the greatest advantage is observed in the cases of severe sea states when platform motions increase (e.g. the LCs in operating region 3). Similar performances are achieved with both the grey and black-box FOWT ROMs. Note that the black-box ROM is identified by considering LC7 (using different random seeds). In fact, the black-box estimation error increases slightly for sea and wind conditions different from LC7. The accuracy of the black-box ROM for LCs different from LC7 demonstrates that non-linear terms of the platform dynamics may be neglected.

https://doi.org/10.5194/wes-2024-144
Preprint. Discussion started: 21 November 2024

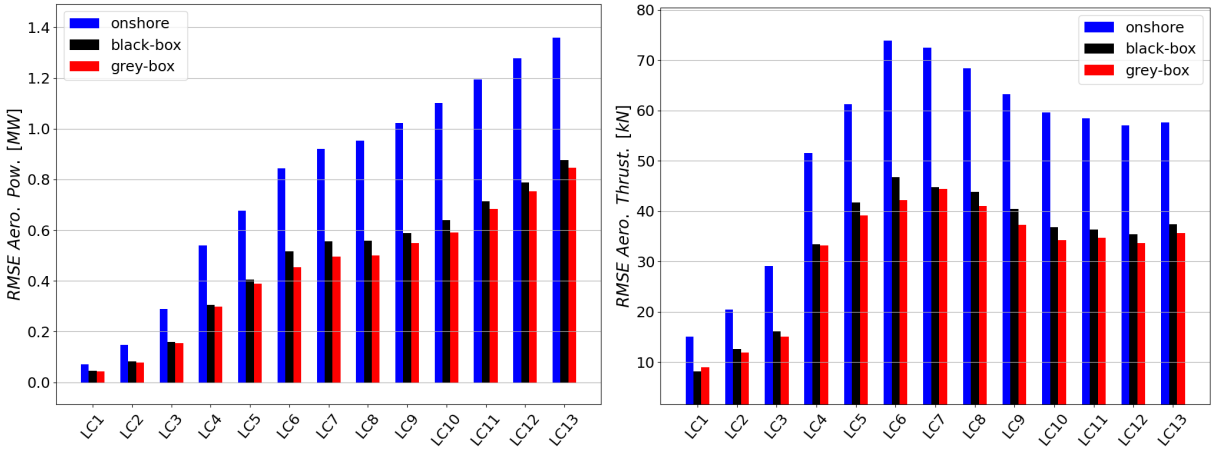

Figure 6. Root Mean Square Error (RMSE) on the estimated aerodynamic power and thrust of the ROMs with respect to the OpenFAST simulations.

Figure 7 depicts the longitudinal nacelle velocity RMSE for the grey and black-box FOWT ROMs. The two ROMs can estimate the nacelle velocity in all the considered LCs with similar accuracy. This suggests that the preference between the two approaches is not to be expressed in terms of accuracy. In the following, the black-box ROM will be used in the ENMPC.

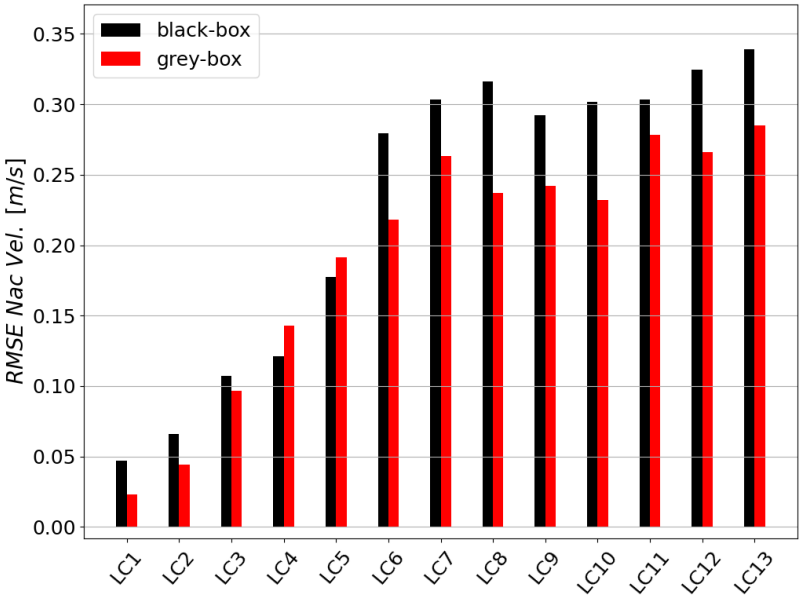

Figure 7. RMSE of the ROMs estimated longitudinal nacelle velocity with respect to the OpenFAST simulations for all the considered LCs.

https://doi.org/10.5194/wes-2024-144
Preprint. Discussion started: 21 November 2024

eawe european academy of wind energy
Open Access WIND ENERGY SCIENCE DISCUSSIONS

4.3 ENMPC tuning

Thanks to the flexibility of the ENMPC, it is easy to define the constraints and objectives of the controller. In this work, two ENMPCs are tested, one for power maximization only ($w = 0$ see section 4.4) and a multi-objective ENMPC for power maximisation and reduction of nacelle velocity ($w = 1$ see section 4.5).

The constraints chosen for both controllers are summarised in table 3. It is the same set of constraints considered in Pustina et al. (2022a), with the addition of a platform surge and a pitch velocity limit. These new constraints are inserted to ensure stable platform dynamics. They are set considering the higher platform velocities obtained using the reference controller in the most severe sea states. They could be modified depending on the wind and condition to improve controller performance.

Constraint	min	max
Rot. Thrust. [kN]	//	700
Gen. Temp. [C°]	//	60
Gen. Pow. [MW]	//	6
Rot. Speed [rpm]	2	15
Blade pitch [deg]	-5	22
Blade pitch vel. [deg/s]	-1.5	1.5
Blade pitch acc. [deg/s^2]	-1.5	1.5
Gen. Tq. [kNm]	0	43
Gen. Tq. der. [kNm/s]	-10	10
Gen. Tq. sec. der. [kNm/s^2]	-3	3
Platf. Surge Vel. [m/s]	-1.5	1.5
Platf. Pitch Vel. [deg/s]	-0.8	0.8

Table 3. Constraints of the optimal control problem.

It is also fundamental to tune the time horizon (i.e. the length of the time window on which the objective function is integrated) and the time update (i.e. the time after when the control law is newly evaluated) of the ENMPC. The same tuning process of Pustina et al. (2022a) is used, and it is not reported here for the sake of conciseness. As in the onshore case, a 1-second update time has resulted sufficient to guarantee good performance. Instead, it was observed that a double time horizon ($T_h = 60$ s with respect to $T_h = 30$ s in the onshore case) is more suitable for the offshore ENMPC. Indeed, with a longer time horizon, low-frequency dynamics (such as platform surge and pitch) becomes more controllable.

The controller is coupled with the OpenFAST fully aeroelastic solver to assess the robustness of the ENMPC with respect to the modeling error. At every update time, the available high-fidelity measurements are used to estimate and impose the initial conditions on the rotor speed, the generator temperature, and the displacements and velocities of the platform. Instead, the mean disk inflow velocity is a non-measurable quantity (at least in a realistic application) and it is not updated (with respect to that, the ENMPC works as a non-linear observer). The time-shifted result of the last update is used as a first guess for optimization

https://doi.org/10.5194/wes-2024-144
Preprint. Discussion started: 21 November 2024

to speed up the numerical solution of the OCP (as explained in the previous section). In our case, $59s$ of the previous control law is available and the time series is extended with the last available values kept constant in the last second.

Some improvements in the OCP numerical formulation have been made with respect to the ENMPC controller developed in Pustina et al. (2022a). First, a non-uniform time grid is adopted, composed of three uniform grids:

- a finer uniform grid for $t < 1s$ with time-step $0.05s$. Since the states are updated with the available measurements at the beginning of this time segment, higher gradients are expected, requiring a finer mesh. This is also the part of the control law that will be actually used due to the update time;
- a transition region for $1s < t < 10s$ with time-step $0.1s$ to avoid high discontinuities in the time-step size;
- a far region for $10s < t < 60s$ with time-step $0.5s$. The ENMPC needs this region to take into account the long-term effects of the evaluated control law. However, a higher time step is adopted to reduce computational time, since a higher estimation error is acceptable in this region.

Following Pustina et al. (2022a), a linear interpolation is used to obtain the control law on the OpenFAST grid (the time-step used in OpenFAST is 0.0125 s).

As in Pustina et al. (2022a), a shift initialization strategy (see section 3.4.1) is adopted for the OCP first guess to reduce computational time.

Moreover, the handling of the constraint is improved with respect to the ENMPC developed in Pustina et al. (2022a) to further accelerate while maintaining the robustness of the controller. The homotopy strategy (see section 3.4.2) is fundamental to ensure ENMPC convergence under all operating conditions. However, the computational time considerably increases because multiple OCPs have to be solved. To speed up the controller, only for the first OCP and in a few cases when the controller does not converge, homotopy is used. Note that when homotopy is disabled, different penalty function parameters (ϵ,h, see fig. 5) are adopted for the different constraints. Indeed, especially in operating region 3, it is fundamental that the generator temperature reaches the limit to ensure the highest admissible power production. For this reason, a steeper penalty function ($\epsilon = 0.001$,$h = 0.001$) is used for the generator temperature, while smoother ones ($\epsilon = 0.001$,$h = 0.01$) are considered for the other constraints where reaching the exact limit is not essential. Moreover, the adoption of smoother penalties, especially for constraints with high modelling error (e.g. rotor thrust), increases the controller robustness. With the described constraint handling, it will be demonstrated in the following sections that the ENMPC is effective under all in operating conditions considered. The constraint violation relaxation strategy (see section 3.4.3) is not necessary and thus not adopted in this work. However, it is implemented in PINS and can be used, if necessary, for a different set of constraints and objective functions.

Thanks to the non-uniform time grid and the novel handling of the constraints, the ENMPC computational time is drastically reduced (about 0.15-0.2s on a workstation PC, that is from 10 to 5 times faster than $1s$, which is the available time frame to complete the replan and to provide the control to the system.).

https://doi.org/10.5194/wes-2024-144
Preprint. Discussion started: 21 November 2024

eawe european academy of wind energy
Open Access WIND ENERGY SCIENCE DISCUSSIONS

4.4 Power maximization ENMPC

First, the single-objective offshore ENMPC is compared to the on-shore ENMPC developed in Pustina et al. (2022a) and to the reference NREL controller to evaluate its performance. Unexpectedly, for all load cases, the onshore ENMPC performs similarly to the offshore ENMPC (see fig. 8). This is due to the fact that, as demonstrated in Pustina et al. (2022a), the onshore ENMPC is robust with respect to wind speed errors. Thus, it is also robust with respect to longitudinal nacelle velocity perturbations. Moreover, the onshore ENMPC ROM contains fewer states, and it is easier for the numerical solver to approach the global optimum of the OCP.

On the contrary, as demonstrated in section 4.2, the more accurate ROM on which the offshore ENMPC is based provides a better estimation of the thrust (see fig. 8). This results in improved capability near the thrust constraint. Note that, as in Pustina et al. (2022a), the thrust constraint ($700kN$) is also slightly violated by the offshore ENMPC because it lacks high-frequency aerodynamic effects.

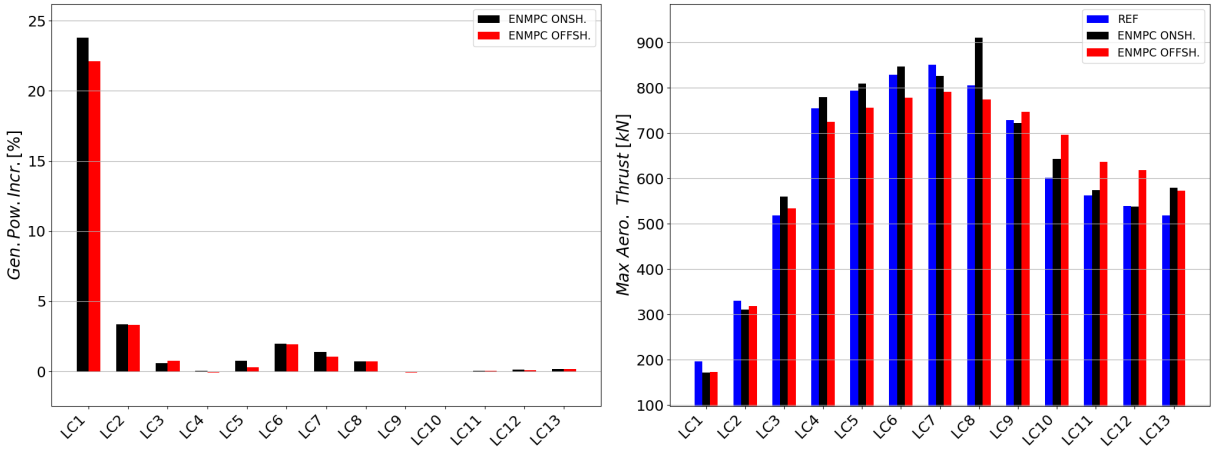

Figure 8. Generated power increment (with respect to the NREL reference controller) and maximum aerodynamic thrust for the reference controller and the onshore and offshore ENMPCs.

This section considers only the single-objective ENMPC, and a pitch and surge velocity of the platform are only constrained and do not directly contribute to in objective function. As a consequence, not only a reduction in longitudinal nacelle velocity (see fig. 9, left) is only expected if the constraint is violated in the offshore ENMPC case, but, in principle, the offshore ENMPC may use an increase of nacelle velocity to improve objective function or (as in this case) to respect other constraints, in particular, that on the maximum thrust. Here, it is evident from LC7 and LC8, for which the longitudinal nacelle velocity of the offshore ENMPC case approaches the constraint, yielding the reduction of maximum thrust observed previously. However, in all the other cases where the maximum thrust is not critical for the considered limit, the longitudinal velocity resulting from the application of the offshore ENMPC is smaller than or equal to that obtained with the other two controllers.

https://doi.org/10.5194/wes-2024-144
Preprint. Discussion started: 21 November 2024

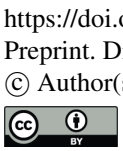

eawe european academy of wind energy
Open Access WIND ENERGY SCIENCE DISCUSSIONS

As expected, the lateral nacelle velocity is conversely similar in the three cases, since it is not included in the offshore ENMPC and has little influence on power production, and the control action is given in terms of collective pitch and generator torque, which have negligible impact on lateral dynamics.

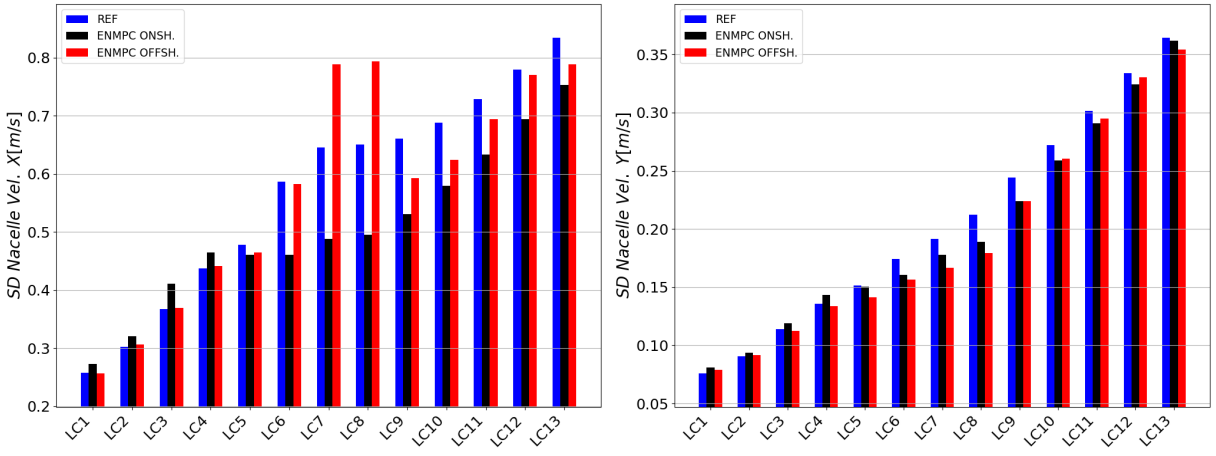

Figure 9. Longitudinal and lateral nacelle velocity standard deviation for the reference controller and the onshore and offshore ENMPCs.

Finally, fig. 10 shows the standard deviation of the blade pitch, which is considered an indicator of the control effort. At about the rated wind speed, the onshore and offshore ENMPCs have a blade pitch standard deviation similar to the reference one, whereas, increasing wind velocity, the reference controller requires a smaller control effort. Therefore, a term depending on the control effort may be added to the objective function if needed. Note that in region 2, the pitch control effort of the standard controller is null, due to the control strategy.

https://doi.org/10.5194/wes-2024-144
Preprint. Discussion started: 21 November 2024

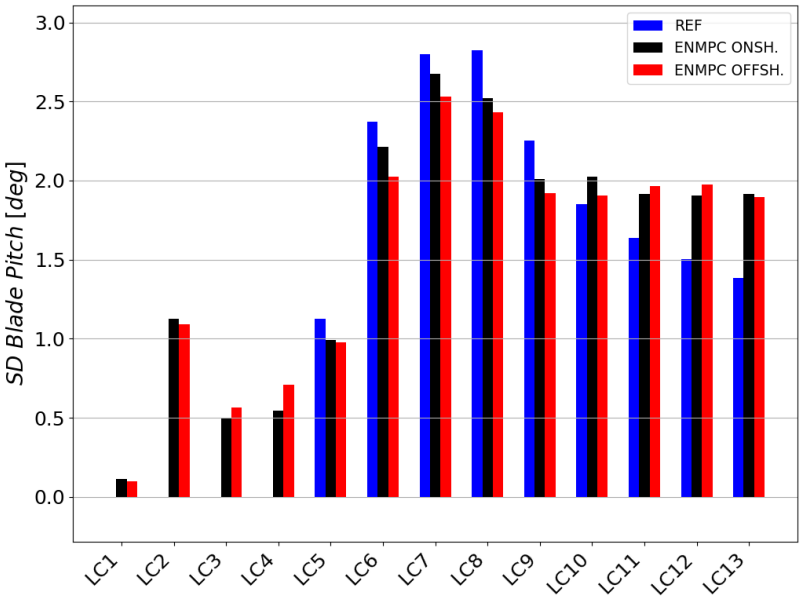

Figure 10. Blade pitch standard deviation for the reference controller and the onshore and offshore ENMPCs.

4.5 Multi-objective ENMPC

Platform motion may significantly affect mooring lines, electric cables, wind turbine vibratory loads, and fatigue. Therefore, reducing the motion of the platform provides several benefits, including capital cost savings on platform and mooring lines. As described in section 3.4, the objective function can be defined by including a longitudinal nacelle velocity term (see eq. (13)), with a relative weight between the two partial objectives.

https://doi.org/10.5194/wes-2024-144
Preprint. Discussion started: 21 November 2024

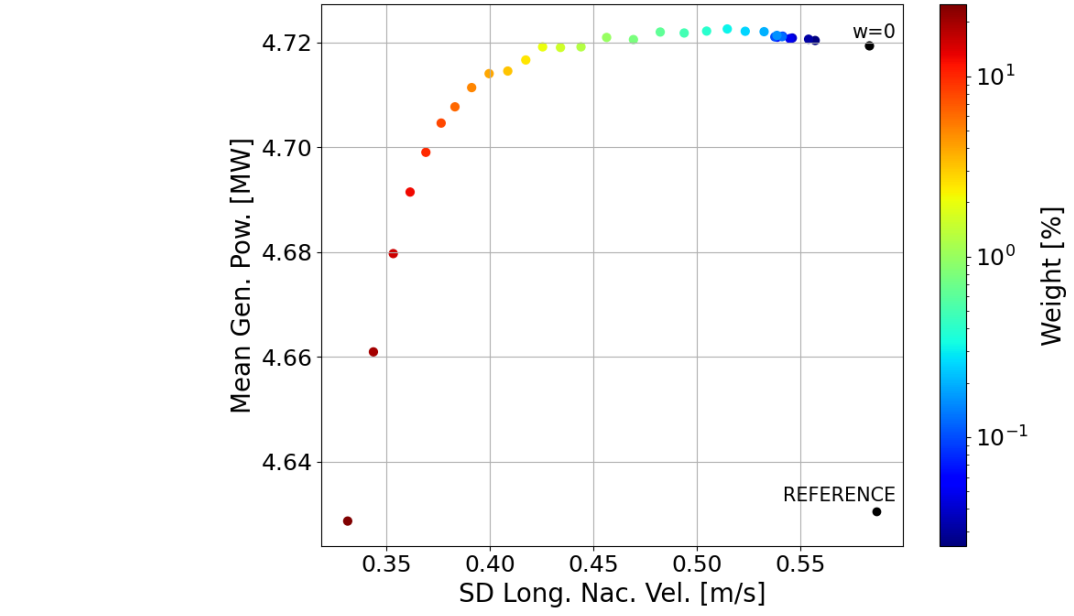

Figure 11. Pareto front of the multi-objective OCP, in the LC6: longitudinal nacelle velocity Standard Deviation on the abscissa axis and mean generated power on the axis of ordinates. The reference point (using the NREL controller) is reported in black. The ENMPC points are coloured considering the weight of the nacelle velocity term.

The weight of the nacelle velocity term is varied from 0.025% to 25% with 30 points logarithmically spaced, and the corresponding results in terms of partial objectives are reported in fig. 11. For conciseness, only the rated wind speed load case (LC6) is considered for this analysis. Note that some slightly dominated points are obtained, especially in the region with lower weights. This is caused by the fact that the ENMPC relies on a gradient-based algorithm that can fall into a local optimum. Generally speaking, in the weight range considered, the percentage variation of the generated power is significantly smaller than that of the standard deviation of the velocity. In particular, up to $w = 2\%$, the power is almost unaffected, whereas, by increasing the weight more than 2%, there is a significant reduction in generated power and a small marginal gain in platform motion. Although it is not exactly the weight value that minimises the distance from the utopia point, 2% is chosen as the weight for all LCs table 2, in that the increase in average power is an objective more relevant than the reduction in the motion of the platform. Alternatively, the two quantities may be made homogeneous by converting them to the same unit, e.g. an economic value.

As expected, a significant reduction in longitudinal nacelle velocity is achieved for all LCs with respect to the reference and the single-objective ENMPC by adopting the multi-objective ENMPC (see fig. 12). The increase in nacelle velocity observed in the single-objective ENMPC for LC7 and LC8 is obviously absent. Moreover, it is confirmed that, for all the LCs, the multi-objective ENMPC gives similar power production to the single-objective ENMPC.

https://doi.org/10.5194/wes-2024-144
Preprint. Discussion started: 21 November 2024

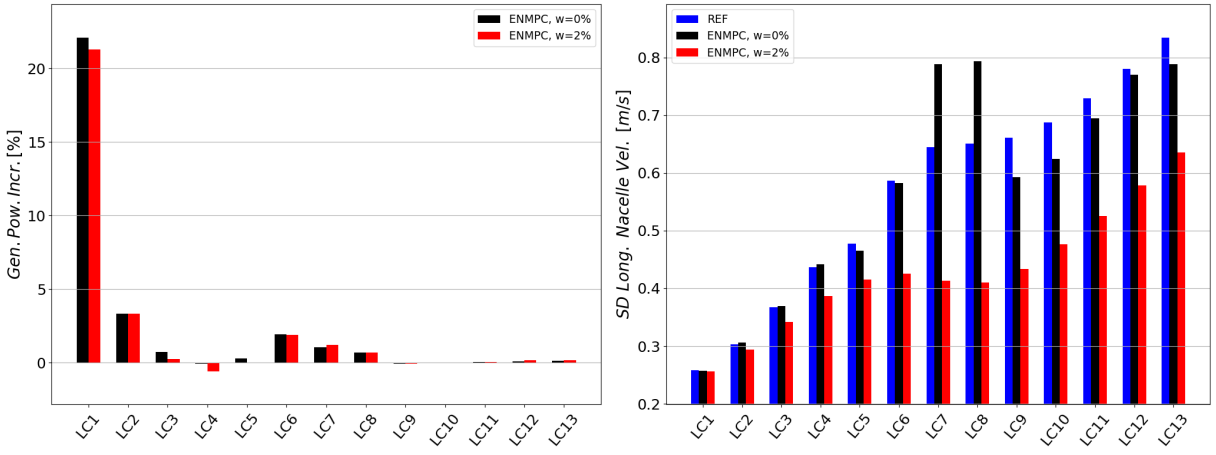

Figure 12. Mean generated power and longitudinal nacelle velocity standard deviation SD for the single-objective ENMPC and for the multi-objective ENMPC ($w = 2\%$).

As the single-objective ENMPC, the multi-objective ENMPC substantially respect the thrust constraint (see fig. 13). However, in operating region 3 (LC8 to LC13), a higher maximum aerodynamic thrust results with the multi-objective ENMPC. This suggests that thrust oscillation and platform motion reduction are conflicting objectives, since platform motion reduction is achieved mainly through thrust. Indeed, the multi-objective ENMPC, for a forward nacelle velocity, increases the blade angle of attack, and thus the thrust, to slow down the nacelle. This causes the fact that, conversely to the reference controller and the single-objective ENMPC, for the multi-objective ENMPC, the reduction in maximum aerodynamic thrust as the wind speed increases is relatively small.

https://doi.org/10.5194/wes-2024-144
Preprint. Discussion started: 21 November 2024

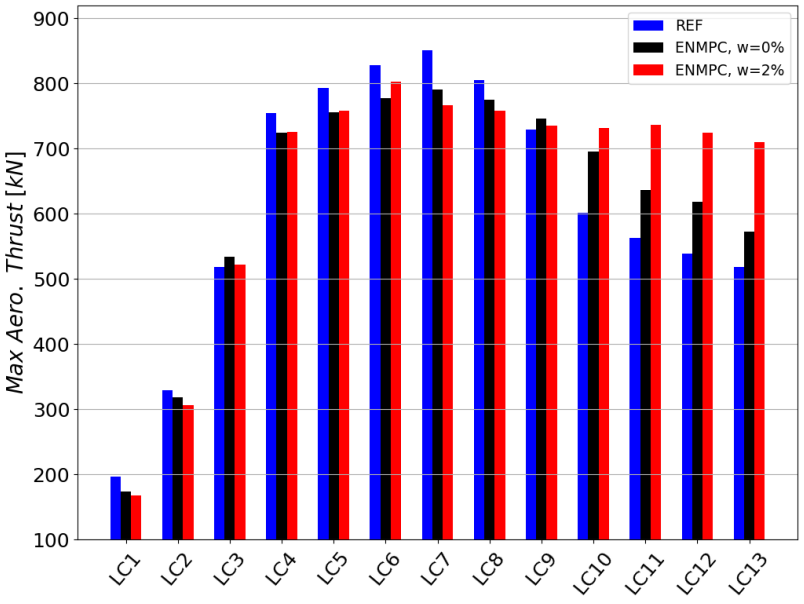

Figure 13. Maximum aerodynamic thrust for the single-objective ENMPC and the multi-objective ENMPC ($w = 2\%$).

Finally, the generated power standard deviation (SD) is analysed as an index of the quality of the power delivered to the grid. In control region 2 (LC1-LC6), the offshore ENMPCs (single- and multi-objective) have similar generated power SD to the NREL reference controller (see fig. 14). In contrast, the offshore ENMPC gives a relatively higher SD because the nacelle velocity is an unmodeled disturbance for the ROM. In operating region 3 (LC7-LC13), all ENMPCs have steadier power production than the reference controller. Indeed, the offshore NREL reference controller is de-tuned with respect to the onshore counterpart to maintain stable platform motion (see section 2), leading to higher oscillations of rotor speed and generated power. Concerning the ENMPCs, as observed in fig. 14, the multi-objective controller has higher power oscillations due to the use of thrust to mitigate platform motion.

https://doi.org/10.5194/wes-2024-144
Preprint. Discussion started: 21 November 2024

eawe european academy of wind energy
Open Access WIND ENERGY SCIENCE DISCUSSIONS

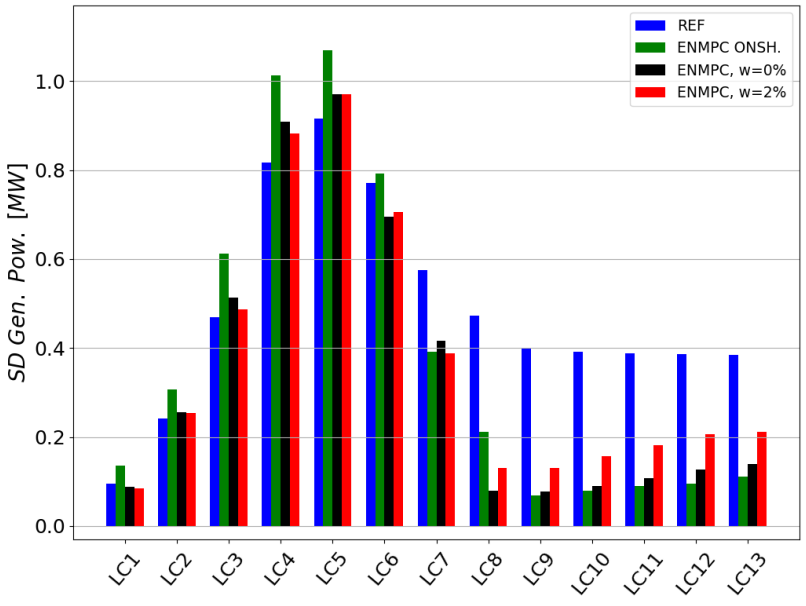

Figure 14. Generated power standard deviation (SD) for the reference NREL controller (REF), the onshore ENMPC, the offshore single-objective ENMPC and the multi-objective ENMPC ($w = 2\%$).

4.6 Robustness of the controller with respect to the wind and wave prediction

The major shortcoming of the developed offshore ENMPC is the need to predict future wind speed and sea diffraction forces on the optimisation time horizon.

Various methodologies are available to estimate or measure the incoming wind. For example, possible options are LIDAR sensors Simley et al. (2012), or wind speed estimation algorithms based on previous measurements Riahy and Abedi (2008). In addition, incoming diffraction forces can be estimated by measuring incoming waves with a wave radar Fucile et al. (2016). However, measuring or predicting incoming wind and waves is not simple. Additional and expensive sensors are required, and the estimation is affected by errors.

Thus, the condition of an absolute lack of knowledge of wind and sea wave prediction is analysed. The surge and pitch diffraction forces are considered null for the entire time horizon, and the wind at the beginning of the time window is considered constant for the entire time horizon. An extended Kalman filter (EKF) Abbas et al. (2021) estimates the current wind speed using only the measurements available on the turbine without the need for a prediction algorithm or nacelle LIDAR. In the FOWT case, the EKF should be modified to account for platform motion. Therefore, to analyse a more realistic condition, a random noise (with amplitude $0.2m/s$) is added to the effective wind speed and then injected into the EKF to evaluate the effect of errors.

As in the onshore case Pustina et al. (2022a), only a small power loss is observed with respect to the perfect prediction case (see fig. 15). In any case, the ENMPC has higher power production than the reference controller.

https://doi.org/10.5194/wes-2024-144
Preprint. Discussion started: 21 November 2024

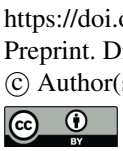

eawe european academy of wind energy
Open Access WIND ENERGY SCIENCE DISCUSSIONS

Instead, a significant increase in the standard deviation of the longitudinal nacelle velocity is observed in the case without prediction (see fig. 15), especially for the most severe sea states. Thus, predicting the diffraction forces seems necessary to control the motion of the platform.

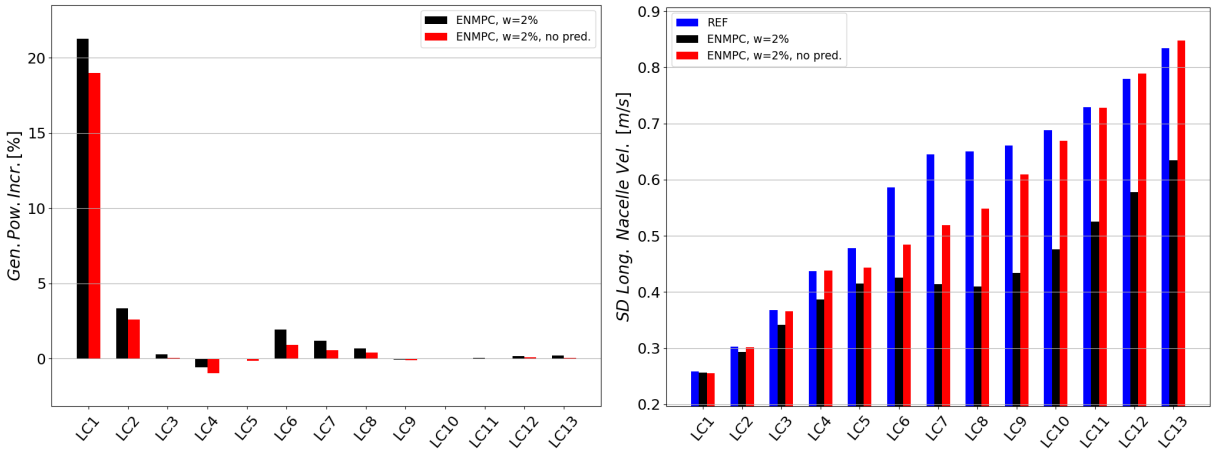

Figure 15. Mean generated power and longitudinal nacelle velocity standard deviation SD for the multi-objective ENMPC ($w = 2\%$) with and without wind and wave forces prediction.

https://doi.org/10.5194/wes-2024-144
Preprint. Discussion started: 21 November 2024

5 Conclusions

A novel Economic Nonlinear Model Predictive Controller has been applied to FOWT for power maximization and platform motion reduction. The controller is validated against high-fidelity simulations considering a comprehensive set of realistic wind and sea state conditions.

The controller is based on a novel ROM specifically tailored for FOWTs from a previously developed ROM for onshore WT. A nonlinear rotor ROM is coupled with a linear platform ROM. Two platform ROMs have been compared, a grey-box and a black-box model.

The FOWTs ROMs are validated against OpenFAST simulations. As a result, a reasonable estimation of the objective functions (aerodynamic power and nacelle velocity) and the constraints (platform velocities, rotor thrust and rotor speed) is achieved with both models. Furthermore, offshore ROM is shown to significantly improve power and thrust estimation with respect to offshore ROM. Finally, the black-box and grey-box platform ROMs have a similar level of accuracy in platform motion estimation for all the considered LCs. The ROMs lack high-frequency phenomena, but this is not relevant to the objectives of the ENMPC.

Then, the ENMPC is coupled with the fully-aeroelastic solver OpenFAST considering a comprehensive set of realistic wind and sea state conditions. First, only the goal of power maximisation is considered for the offshore ENMPC, and the controller is compared to the offshore ENMPC and the reference NREL controller Jonkman (2010). It is demonstrated that the onshore ENMPC can be applied for FOWT and has similar power production to the offshore ENMPC. However, the onshore ENMPC gives higher thrust peaks than the offshore ENMPC, which is based on a ROM, which is more accurate in the thrust estimation.

Then, the multi-objective ENMPC for power maximisation and longitudinal nacelle velocity reduction is tested. For the rated wind speed case, the Pareto front is evaluated to select the optimal weight for the nacelle speed term. Then, the multi-objective ENMPC is compared to the onshore ENMPC and the offshore ENMPC for all the considered LCs. As a result, the multi-objective ENMPC can maintain a similar power production to the power maximisation ENMPC and reduce the longitudinal nacelle velocity. Concerning produced power quality, especially in control region 3, it is higher than that resulting from in use of the reference controller for all the ENMPCs. In the future, the objective function may be modified to take into account power fluctuations in order to improve more the power quality. This can be done easily in the MPC framework, e.g., by introducing a term depending on the standard deviation of power.

Finally, considering the difficulty in predicting the sea diffraction forces and the incoming wind, the performances of the multi-objective ENMPC are assessed in the case of the absence of these predictions. The ENMPC without predictions has power production similar to that of the perfect prediction case. However, predicting the diffraction forces (in the literature, both first- and second-order ones have been demostrated to affect platform motion) seems necessary to reduce the longitudinal nacelle velocity. To overcome this issue, the authors are working on an Extended Kalman Filter for FOWTs capable of estimating wind and sea diffraction forces. The fact that the knowledge of the current value of mean wind on the disc is sufficient for the controller application and the exact knowledge on the incoming wind is not necessary, is very positive, since the platform motion is know to depends also on the very low-frequency content of the wind spectrum (not included in the Kaimal spectrum used here), which in the real application would be very complex to be predicted also by using a LIDAR.

https://doi.org/10.5194/wes-2024-144
Preprint. Discussion started: 21 November 2024

Comparing the results with those present in the literature, the conflicting nature of power augmentation and motion reduction goal have been confirmed by the existence of a convex Pareto front. Many areas of investigation and many possible improvements are envisaged. The model and subsequently the controller may be extended to include yaw motion and gyroscopic effects to deal with misaligned wind and waves.

Concerning future experimental validation, in the authors' opinion the next step is to implement the controller on an actual wind turbine. Indeed, the use of small models is quite complex, since it requires a coupled hydro-wind facility and the scale factor would be compulsorily high, making it impossible to respect the similarity. On the other hand, the controller itself is based on measurements and actuators already available on the actual wind turbines, avoiding the need of dedicated hardware. Nevertheless, the use of dedicated hardware for the estimation of wind speed and wave height could increase power production.

Competing interests

The contact author has declared that none of the authors has any competing interests

Acknowledgments

The research activity is supported by the Italian "Ministero dell'Ambiente e della Sicurezza Energetica" under the Grant Agreement "RdS PTR 2022–2024 - Energia elettrica dal mare".

https://doi.org/10.5194/wes-2024-144
Preprint. Discussion started: 21 November 2024

eawe european academy of wind energy
Open Access WIND ENERGY SCIENCE DISCUSSIONS

References

Abbas, N., Zalkind, D., Pao, L., and Wright, A.: A Reference Open-Source Controller for Fixed and Floating Offshore Wind Turbines, Wind Energy Science Discussions, 2021, 1–33, https://doi.org/10.5194/wes-2021-19, 2021.

Aboutalebi, P., M'zoughi, F., Garrido, I., and Garrido, A. J.: Performance analysis on the use of oscillating water column in barge-based floating offshore wind turbines, Mathematics, 9, 475, 2021.

Allen, C., Viselli, A., Dagher, H., Goupee, A., Gaertner, E., Abbas, N., Hall, M., and Barter, G.: Definition of the UMaine VolturnUS-S Reference Platform Developed for the IEA Wind 15-Megawatt Offshore Reference Wind Turbine, Tech. rep., International Energy Agency, https://www.nrel.gov/docs/fy20osti/76773.pdf, 2020.

Bagherieh, O. and Nagamune, R.: Gain-scheduling control of a floating offshore wind turbine above rated wind speed, Control Theory and Technology, 13, 160–172, 2015.

Biral, F., Bertolazzi, E., and Bosetti, P.: Notes on numerical methods for solving optimal control problems, IEEJ Journal of Industry Applications, 5, 154–166, 2016.

Borg, M., Walkusch Jensen, M., Urquhart, S., Andersen, M. T., Thomsen, J. B., and Stiesdal, H.: Technical definition of the Tetraspar demonstrator floating wind turbine foundation, Energies, 13, 4911, 2020.

Burton, T., Jenkins, N., Sharpe, D., and Bossanyi, E.: Wind energy handbook, John Wiley & Sons, 2011.

Dong, J. and Viré, A.: The aerodynamics of floating offshore wind turbines in different working states during surge motion, Renewable Energy, 195, 1125–1136, https://doi.org/https://doi.org/10.1016/j.renene.2022.06.016, 2022.

Duarte, T., Gueydon, S., Jonkman, J., and Sarmento, A.: Computation of wave loads under multidirectional sea states for floating offshore wind turbines, in: International Conference on Offshore Mechanics and Arctic Engineering, vol. 45547, p. V09BT09A023, American Society of Mechanical Engineers, 2014.

Durakovic, A.: BayWa r.e. Unveils Subsidy-Free Floating Wind Project Offshore Portugal, https://www.offshorewind.biz/2022/10/17/baywa-r-e-unveils-subsidy-free-floating-wind-project-offshore-portugal/, 2017.

Fischer, T., De Vries, W., and Schmidt, B.: UpWind Design Basis (WP4: Offshore foundations and support structures), Tech. rep., TUDelft, 2010.

Fleming, P. A., Pineda, I., Rossetti, M., Wright, A. D., and Arora, D.: Evaluating methods for control of an offshore floating turbine, in: International Conference on Offshore Mechanics and Arctic Engineering, vol. 45547, p. V09BT09A019, American Society of Mechanical Engineers, 2014.

Fu, S., Jin, Y., Zheng, Y., and Chamorro, L. P.: Wake and power fluctuations of a model wind turbine subjected to pitch and roll oscillations, Applied Energy, 253, 113 605, 2019.

Fucile, F., Ludeno, G., Serafino, F., Bulian, G., Soldovieri, F., and Lugni, C.: Some challenges in recovering wave features from a wave radar system, in: The 26th International Ocean and Polar Engineering Conference, OnePetro, 2016.

Gaertner, E., Rinker, J., Sethuraman, L., Zahle, F., Anderson, B., Barter, G., Abbas, N., Meng, F., Bortolotti, P., Skrzypinski, W., Scott, G., Feil, R., Bredmose, H., Dykes, K., Sheilds, M., Allen, C., and Viselli, A.: Definition of the IEA 15-megawatt Offshore Reference Wind Turbine, Tech. rep., International Energy Agency, https://www.nrel.gov/docs/fy20osti/75698.pdf, 2020.

Gennaretti, M., Gori, R., Serafini, J., Cardito, F., and Bernardini, G.: Identification of Rotor Wake Inflow Finite-State Models for Flight Dynamics Simulations, CEAS Aeronautical Journal, 8, 209–230, 2017.

Gros, S. and Diehl, M.: Numerical Optimal Control (Draft), https://www.syscop.de/files/2020ss/NOC/book-NOCSE.pdf, 2022.

https://doi.org/10.5194/wes-2024-144
Preprint. Discussion started: 21 November 2024

Hall, M.: MoorDyn—Users Guide, Department of Mechanical Engineering, University of Maine: Orono, ME, USA, 2015.

Hara, N., Tsujimoto, S., Nihei, Y., Iijima, K., and Konishi, K.: Experimental validation of model-based blade pitch controller design for floating wind turbines: system identification approach, Wind energy, 20, 1187–1206, 2017.

Hasselmann, K., Barnett, T. P., Bouws, E., Carlson, H., Cartwright, D. E., Enke, K., Ewing, J. A., Gienapp, H., Hasselmann, D. E., , Kruseman, P., Meerburg, A., Mller, P., Olbers, D. J., Richter, K., Sell, W., and Walden, H.: Measurements of wind-wave growth and swell decay during the Joint North Sea Wave Project (JONSWAP), Ergnzungsheft zur Deutschen Hydrographischen Zeitschrift Reihe, A8, 1973.

Henriksen, L. C., Poulsen, N. K., and Hansen, M. H.: Nonlinear model predictive control of a simplified wind turbine, IFAC Proceedings Volumes, 44, 551–556, 2011.

IRENA: Tracking the impacts of innovation: Offshore wind as a case study, International Renewable Energy Agency Abu Dhabi, 2021.

James, R. and Ros, M. C.: Floating offshore wind: market and technology review, Tech. rep., The Carbon Trust, 2015.

Jard, T. and Snaiki, R.: Real-time repositioning of floating wind turbines using model predictive control for position and power regulation, Wind, 3, 131–150, 2023.

Jena, D. and Rajendran, S.: A review of estimation of effective wind speed based control of wind turbines, Renewable and Sustainable Energy Reviews, 43, 1046–1062, 2015.

Jonkman, B. J. and Buhl Jr, M. L.: TurbSim user's guide, Tech. rep., National Renewable Energy Lab.(NREL), Golden, CO (United States), 2006.

Jonkman, J.: Definition of the Floating System for Phase IV of OC3, Tech. rep., National Renewable Energy Lab.(NREL), Golden, CO (United States), 2010.

Jonkman, J.: The new modularization framework for the FAST wind turbine CAE tool, in: 51st AIAA Aerospace Sciences Meeting including the New Horizons Forum and Aerospace Exposition, p. 202, 2013.

Jonkman, J., Butterfield, S., Musial, W., and Scott, G.: Definition of a 5-MW reference wind turbine for offshore system development, Tech. rep., National Renewable Energy Lab.(NREL), Golden, CO (United States), 2009.

Lackner, M. A.: Controlling platform motions and reducing blade loads for floating wind turbines, Wind Engineering, 33, 541–553, 2009.

Larsen, T. J. and Hanson, T. D.: A method to avoid negative damped low frequent tower vibrations for a floating, pitch controlled wind turbine, Journal of Physics: Conference Series, 75, 012 073, 2007.

Leishman, G. J.: Principles of helicopter aerodynamics, Cambridge Aerospace Series, 2016.

Liberzon, D.: Calculus of variations and optimal control theory, Princeton university press, 2011.

Lio, W. H., Rossiter, J., and Jones, B. L.: A review on applications of model predictive control to wind turbines, in: 2014 UKACC International Conference on Control (CONTROL), pp. 673–678, https://doi.org/10.1109/CONTROL.2014.6915220, 2014.

López-Queija, J., Robles, E., Jugo, J., and Alonso-Quesada, S.: Review of control technologies for floating offshore wind turbines, Renewable and Sustainable Energy Reviews, 167, 112 787, 2022.

Lydia, M., Kumar, S. S., Selvakumar, A. I., and Kumar, G. E. P.: A comprehensive review on wind turbine power curve modeling techniques, Renewable and Sustainable Energy Reviews, 30, 452–460, 2014.

Masson-Delmotte, V., Zhai, P., A., Pirani, Connors, S., Péan, C., Berger, S., Caud, N., Chen, Y., Goldfarb, L., Gomis, M., Huang, M., Leitzell, K., Lonnoy, E., Matthews, J., Maycock, T., Waterfield, T., Yelekci, O., Yu, R., and (eds.), B. Z.: IPCC, 2021: Climate Change 2021: The Physical Science Basis. Contribution of Working Group I to the Sixth Assessment Report of the Intergovernmental Panel on Climate Change, Tech. rep., IPCC, 2021a.

https://doi.org/10.5194/wes-2024-144
Preprint. Discussion started: 21 November 2024

Masson-Delmotte, V., Zhai, P., A., Pirani, Connors, S., Péan, C., Berger, S., Caud, N., Chen, Y., Goldfarb, L., Gomis, M., Huang, M., Leitzell, K., Lonnoy, E., Matthews, J., Maycock, T., Waterfield, T., Yelekci, O., Yu, R., and (eds.), B. Z.: IPCC, 2021:Summary for policymakers, Tech. rep., IPCC, 2021b.

Moriarty, P. J. and Hansen, A. C.: AeroDyn theory manual, Tech. rep., National Renewable Energy Lab., Golden, CO (US), 2005.

Namik, H. and Stol, K.: Individual blade pitch control of a spar-buoy floating wind turbine, IEEE transactions on control systems technology, 22, 214–223, 2013.

Pitt, D. M. and Peters, D. A.: Theoretical prediction of dynamic inflow derivatives, Vertica, 5, 1981.

Pontryagin, L. S.: Mathematical theory of optimal processes, CRC press, 1987.

Pustina, L., Lugni, C., Bernardini, G., Serafini, J., and Gennaretti, M.: Control of power generated by a floating offshore wind turbine perturbed by sea waves, Renewable and Sustainable Energy Reviews, 132, 109 984, 2020.

Pustina, L., Pasquali, C., Serafini, J., Lugni, C., and Gennaretti, M.: Individual blade pitch control for alleviation of vibratory loads on floating offshore wind turbines, Proceedings of Proceedings of the ASME 2021 40th International Conference on Ocean, Offshore and Arctic Engineering, 2021.

Pustina, L., Biral, F., and Serafini, J.: A novel Economic Nonlinear Model Predictive Controller for power maximisation on wind turbines, Renewable and Sustainable Energy Reviews, 170, 112 964, 2022a.

Pustina, L., Serafini, J., and Biral, F.: Robustness of an Economic Nonlinear model predictive control for wind turbines under changing environmental and wear conditions, IEEE Control Systems Letters, 7, 769–774, 2022b.

Pustina, L., Serafini, J., Pasquali, C., Solero, L., Lidozzi, A., and Gennaretti, M.: A novel resonant controller for sea-induced rotor blade vibratory loads reduction on floating offshore wind turbines, Renewable and Sustainable Energy Reviews, 173, 113 073, https://doi.org/https://doi.org/10.1016/j.rser.2022.113073, 2023.

Riahy, G. and Abedi, M.: Short term wind speed forecasting for wind turbine applications using linear prediction method, Renewable energy, 33, 35–41, 2008.

Robertson, A., Jonkman, J., Masciola, M., Song, H., Goupee, A., Coulling, A., and Luan, C.: Definition of the semisubmersible floating system for phase II of OC4, Tech. rep., National Renewable Energy Lab.(NREL), Golden, CO (United States), 2014.

Salic, T., Charpentier, J. F., Benbouzid, M., and Le Boulluec, M.: Control strategies for floating offshore wind turbine: challenges and trends, Electronics, 8, 1185, 2019.

Sarkar, S., Fitzgerald, B., and Basu, B.: Nonlinear model predictive control to reduce pitch actuation of floating offshore wind turbines, IFAC-PapersOnLine, 53, 12 783–12 788, 2020.

Schlipf, D., Schlipf, D. J., and Kühn, M.: Nonlinear model predictive control of wind turbines using LIDAR, Wind energy, 16, 1107–1129, 2013.

Shah, K. A., Li, Y., Nagamune, R., Zhou, Y., and Ur Rehman, W.: Platform motion minimization using model predictive control of a floating offshore wind turbine, Theoretical and Applied Mechanics Letters, 11, 100 295, https://doi.org/https://doi.org/10.1016/j.taml.2021.100295, 2021.

Simley, E., Pao, L., Kelley, N., Jonkman, B., and Frehlich, R.: Lidar wind speed measurements of evolving wind fields, in: 50th AIAA aerospace sciences meeting including the new horizons forum and aerospace exposition, p. 656, 2012.

Sun, H., Gao, X., and Yang, H.: A review of full-scale wind-field measurements of the wind-turbine wake effect and a measurement of the wake-interaction effect, Renewable and Sustainable Energy Reviews, 132, 110 042, 2020.

https://doi.org/10.5194/wes-2024-144
Preprint. Discussion started: 21 November 2024

Thiery, F., Hara, N., and Konishi, K.: Model predictive control for floating offshore wind turbines with failure compensation using individual blade pitch control, in: 2015 15th International Conference on Control, Automation and Systems (ICCAS), pp. 1469–1473, IEEE, 2015.

Van Overschee, P. and De Moor, B.: Subspace identification for linear systems: Theory—Implementation—Applications, Springer Science & Business Media, 2012.

Verhaegen, M.: Identification of the deterministic part of MIMO state space models given in innovations form from input-output data, Automatica, 30, 61–74, 1994.

VV.AA.: IEC 61400-3 (Draft January 2006), Wind turbines-Part 3: Design requirements for offshore wind turbines, Tech. rep., International Electrotechnical Commission, Geneva, Switzerland, 2006.

VV.AA.: MATLAB version 9.7.0.1216025 (R2019b) Update 1, Natick, Massachusetts, 2019a.

VV.AA.: T, Tech. rep., International Renewable Energy Agency, 2019b.

VV.AA.: Floating offshore wind-power generating platform, https://www.edp.com/en/innovation/windfloat, 2022.

Wen, B., Dong, X., Tian, X., Peng, Z., Zhang, W., and Wei, K.: The power performance of an offshore floating wind turbine in platform pitching motion, Energy, 154, 508–521, 2018.

Wu, Z. and Li, Y.: Hybrid model predictive control of floating offshore wind turbines with artificial muscle actuated mooring lines, Journal of Dynamic Systems, Measurement, and Control, 144, 051 003, 2022.

Yan, Z., Hall, J., and Chen, D.: MIMO control of wind turbine using direct shooting method, in: 2013 American Control Conference, pp. 3655–3660, IEEE, 2013.

Yang, C., Chen, P., Cheng, Z., Xiao, L., Chen, J., and Liu, L.: Aerodynamic damping of a semi-submersible floating wind turbine: an analytical, numerical and experimental study, Ocean Engineering, 281, 114 826, 2023.

Yu, W., Lemmer, F., Schlipf, D., Cheng, P. W., Visser, B., Links, H., Gupta, N., Dankemann, S., Counago, B., and Serna, J.: Evaluation of control methods for floating offshore wind turbines, in: Journal of Physics: Conference Series, vol. 1104, p. 012033, IOP Publishing, 2018.

Zhang, C. and Plestan, F.: Power and motion control of a floating wind turbine: an original approach based on adaptive second order sliding mode control, in: IFAC World Congress, 2020.